

Large-orbital-degeneracy expansion for the lattice Anderson model

A. J. Millis* and P. A. Lee

Department of Physics, Massachusetts Institute of Technology, Cambridge, Massachusetts 02139

(Received 11 July 1986)

We study the low-temperature Anderson lattice Hamiltonian via an “auxiliary-boson” $1/N$ expansion that generalizes to a lattice an approach previously used to study one Anderson impurity. We set up the formalism needed and show that infrared divergences cancel in physical quantities. We show that as far as low-energy excitations are concerned the model behaves like a “heavy” Fermi liquid with a Fermi temperature determined essentially by the one-impurity Kondo temperature. We compute thermodynamic quantities including the Wilson ratio, we study the electron wave functions in the ground state of the lattice and compare them with the wave functions in the ground state of the one-impurity problem, we discuss the question of which physical quantities involve the “mass enhancement” present in the thermodynamics, we compute the spin-spin and density-density correlation functions, and we discuss the frequency- and temperature-dependent conductivity, obtaining results in qualitative agreement with experiment.

I. INTRODUCTION

In this paper we report some results of a study of the low-temperature properties of the lattice Anderson Hamiltonian, in the “Kondo limit,” where it describes a band of nearly free electrons hybridizing with a very highly correlated band of f electrons. In the absence of this hybridization the f electrons would be confined, one to a site, in localized orbitals far below the Fermi energy. In this limit, the model is believed to contain the essential physics of the currently interesting “heavy fermion” metals. For a review of previous work on this model, see Ref. 1. In this paper we use a “slave-boson” (or “auxiliary-boson”) $1/N$ expansion that is a simple generalization of a technique previously applied to the one-impurity Anderson model.²⁻⁴ The formalism yields a systematic expansion in a small parameter ($1/N$); within this expansion we study thermodynamic quantities (specific-heat coefficient γ , susceptibility χ , Wilson ratio $R = \chi/\gamma$, and compressibility $dn/d\mu$) to leading and next-to-leading order in $1/N$. Further, we are able to clarify the nature of the ground state for the lattice and its relation to the ground state of the one-impurity problem, thus illuminating an objection that was made⁵ to the concept of a “Kondo lattice.” Finally, we give some results for dynamic quantities [spin-spin and density-density correlation functions and conductivity $\sigma(\omega, T)$] for small frequencies ω and temperatures T . The low-frequency limit of the dynamic quantities is of interest also because it sheds light on the nature of the low-temperature “Fermi liquid” ground state that we find.

The slave-boson technique was applied to the lattice Anderson model previously.^{6,7} However, in the previous work a mean-field approximation was always made, and only C , χ , and R were studied. (For C , χ , and R the mean-field and leading order in $1/N$ results are the same.) After the bulk of the work reported here was completed, we became aware of other work⁸ employing a slave-boson large- N expansion for the Anderson lattice. The model of

Ref. 8 is essentially identical to that considered in this paper; however, the “radial gauge” formulation of the problem was used, instead of the Cartesian gauge formulation used in the present paper. Essentially the same thermodynamic results as those obtained here were derived via an interesting and useful connection with the conventional Landau Fermi-liquid theory. Also, the existence of a $T^3 \ln T$ term in the specific heat was pointed out.

The lattice Anderson model has also been studied in various other approximations, including the Gutzwiller method^{9,10} and various extensions^{11,12} of results for the one-impurity Anderson model. These approximations are physically appealing and may be applied to more realistic models than that considered here. However, the approximations are uncontrolled and only thermodynamic results have been obtained from these approaches. The calculation of correlation functions in these models would be very difficult. Also, the extension of the one-impurity results to the lattice requires assumptions which have been criticized.⁵ The need for a systematic expansion, using a formalism that can deal with both thermodynamic and dynamic quantities, is clear.

The rest of the paper is organized as follows. In Sec. II we discuss our model, formalism, and central approximation. Then in Sec. III we discuss the thermodynamics. Section IV contains a discussion of the ground state of the lattice and a comparison with that of the impurity, and gives some results for spin-spin and density-density correlation functions. In Sec. V we discuss $\sigma(\omega, T)$. Throughout, we compare our approach with the other available analyses of the Anderson lattice Hamiltonian. Subsequent papers will analyze a superconducting instability of the model and consider the density-fluctuation collective modes in more detail.

II. FORMALISM

In this section we present the model and formalism which will be used in subsequent sections. We wish to study the $U = \infty$ Anderson model. This describes an

essentially structureless band of d electrons (bandwidth W , operator $c_{k\sigma}$, energy ε_k) which hybridize with a localized (hence dispersionless) set of f orbitals (operator f_{im} , energy E_{0m}), subject to the constraint that the number of electrons on the f orbitals of any site i is less than or equal to one. Here k labels crystal momentum, σ is conduction-electron spin, i labels lattice sites, and m indexes the various f states on a given site. The Hamiltonian and constraint are

$$H_A = \sum_{k\sigma} \varepsilon_{k\sigma} c_{k\sigma}^\dagger c_{k\sigma} + \sum_{i,m} E_{0m} f_{im}^\dagger f_{im} + \sum_{k,i,m,\sigma} [V(k,m,\sigma) e^{ik \cdot R_i} c_{k\sigma} f_{im} + \text{H.c.}] \quad (2.1a)$$

$$\left\langle \sum_m f_{im}^\dagger f_{im} \right\rangle \equiv \langle n_f^i \rangle \leq 1. \quad (2.1b)$$

The energies $\varepsilon_{k\sigma}$ and E_{0m} are measured from the chemical potential μ . For the explicit computations, we use

$$\varepsilon_{k\sigma} = k^2/2m - \mu = \frac{k^2 - k_h^2}{2m}, \quad (2.2)$$

where m is the c -electron band mass. The energy of the bottom of the band relative to μ is $-W$. $V(k,m,\sigma)$ is a hybridization matrix element. One may estimate the broadening Δ_0 of the f level due to hybridization with the d electrons as

$$\Delta_0 \sim \rho_0 V_0^2,$$

where V_0^2 is some average value for $V(k,m,\sigma)$ and $\rho_0 = mk_h/2\pi^2$ is the c -electron density of states at $\varepsilon_k = \mu$. We are interested in the Kondo limit, in which

$$E_{0m} < 0, \quad (2.3a)$$

$$|E_{0m}| \gg \Delta_0. \quad (2.3b)$$

In this limit the f levels, indexed by m , would all be fully occupied, were it not for the constraint (2.1b). However, Eqs. (2.1) and (2.3) imply that the f occupancy on any site is less than, but nearly equal to 1. In this limit, one might expect each f site to have a definite spin, and one might further expect a lattice of such f sites to order magnetically at low temperatures. However, in the one-impurity case [in which the sum over lattice sites i in Eqs. (2.1) is restricted to one site, conventionally taken to be the origin], it is known¹³ that the Kondo effect, which involves resonant scattering at low temperatures between the spin on the f site and c electrons with energies near the chemical potential, leads to a nonmagnetic ground state in which the spin on the f site is compensated. It is now believed that something analogous to the one-impurity Kondo effect occurs in the lattice problem, and leads to a nonmagnetic ground state. We study this ground state in this paper.

The key feature in the Hamiltonian is the constraint, Eq. (2.1b). This is difficult to deal with because (a) it is an inequality and (b) the dynamics generated by Eqs. (2.1) do not preserve the constraint, Eq. (2.1b): $[H, n_f^i] \neq 0$. One convenient way to proceed depends on a key insight due to Coleman,² Read and Newns,³ and Barnes.⁴ One introduces a new boson field b_i^\dagger , which creates a hole on the f

orbitals on site i , and one rewrites the hybridization term as

$$\sum_{k,i,m,\sigma} [V(k,m,\sigma) e^{ik \cdot R_i} c_{k\sigma}^\dagger f_{im} b_i^\dagger + \text{H.c.}]$$

and replaces the constraint, Eq. (2.1b), by

$$Q_i = n_f^i + n_b^i = 1. \quad (2.4)$$

In Eq. (2.4), Q_i , n_f^i and n_b^i are operators.

The resulting Hamiltonian has the same matrix elements as Eq. (2.1) provided that one stays within the manifold of states such that Eq. (2.4) is satisfied.² Further, the resulting Hamiltonian is amenable to solution by conventional quantum field-theoretical techniques, including a $1/N$ expansion. To motivate our $1/N$ expansion, we examine the hybridization term.

It is convenient to write the f electrons at site i in terms of a basis of definite total angular momentum J . $J = L + S$ where S is spin and L is orbital angular momentum (referred to site i). Typically, only one value of J is relevant. Then m indexes the states of definite J , $-J \leq m \leq J$. If the conduction electrons are expanded in terms of a basis set of spherical harmonics centered on a site i , only those conduction electrons of total angular momentum J and quantum number m will hybridize with the state created by f_{im}^\dagger . Further, if the conduction band is structureless, J and m will be good quantum numbers for the free conduction electron Hamiltonian, and all c -electron states of a given J and radial wave vector but different m will have the same energy. Thus, in the single-impurity Anderson Hamiltonian the c electrons with $J' \neq J$ decouple from the problem and one is left with a model in which $N = 2J + 1$ degenerate bands of conduction electrons hybridize with N degenerate f orbitals. It is then easy to see that this model possesses a $1/N$ expansion.^{2,3} (Note that crystal-field splitting of the f level can be incorporated into the model. A $1/N$ expansion still results, but with N equal to the degeneracy of the lowest crystal-field-split multiplet; thus $N < 2J + 1$.)

This expansion is not available in the lattice problem because J is not conserved as conduction electrons propagate from site to site. An electron in a state of definite L (referred to site I) will be in a superposition of states of many different L 's if the origin is referred to some other site i' . Keeping track of how J varies as c electrons propagate through a lattice would be very complicated. Thus, as a first step towards understanding the Hamiltonian and constraint, Eqs. (2.1c) and (2.1b), we propose to ignore these complexities and instead assume that both c - and f -electron states are characterized by a spatial coordinate and an N -fold degenerate "spin" quantum number m , where

$$-J \leq m \leq J$$

and

$$N = 2J + 1.$$

The quantum number m is conserved both in hybridization and c -electron propagation through the lattice.

The problem then possesses a $1/N$ expansion analogous to that in the single-impurity problem. The Hamiltonian

is written

$$H' = \sum_{k,m} \varepsilon_k c_{km}^\dagger c_{km} + E_{om} f_{km}^\dagger f_{km} + V \sum_{k,q,m} (c_{km}^\dagger f_{qm} b_{q-k}^\dagger + \text{H.c.}) . \quad (2.5)$$

We have chosen the hybridization matrix element to be structureless for simplicity. Note that

$$[H', Q_i] = 0 . \quad (2.6)$$

Thus, the time evolution generated by H' preserves the constraint, Eq. (2.4), so that it is only necessary to enforce it at one particular time. To do this it is convenient to introduce another time-independent field λ_i and a new term in the Hamiltonian, so $H \rightarrow H + H_{\text{new}}$, with

$$H_{\text{new}} = \sum_i \lambda_i \left[\sum_m f_{im}^\dagger f_{im} + b_i^\dagger b_i - Q_i \right] . \quad (2.7)$$

Note that the equation of motion of the λ field in the Heisenberg picture is

$$0 = \frac{\partial \lambda_i}{\partial t} = [H, \lambda_i] = \sum_m f_{im}^\dagger f_{im} + b_i^\dagger b_i - Q_i . \quad (2.8)$$

Thus the constraint (2.4) is preserved by the dynamics of H' . We have also checked this explicitly—see below.

We now study H by a $1/N$ expansion about a mean-field solution, as was previously done for the one-impurity problem. In the one-impurity problem, the expansion for the low-temperature properties has been formulated in two different, but ultimately equivalent, ways. One, which we do not use here, is often referred to as the radial gauge. In this approach one defines the magnitude r_i and phase θ_i of the boson field at lattice site i via

$$b_i = r_i e^{i\theta_i} , \\ b_i^\dagger = r_i e^{-i\theta_i} .$$

Then, one defines a new f operator, which we denote f' , via

$$f'_i = f_i e^{i\theta_i} , \\ f_i^\dagger = f_i'^\dagger e^{-i\theta_i} .$$

After making these changes of variable, one discovers that the theory may be written in terms of the fields c , f' , r , and ϕ , where

$$\phi_i = \partial \theta_i / \partial t + \lambda_i .$$

Neither the static part of θ_i nor the fluctuating part of the Lagrange multiplier field λ_i appear explicitly.

This radial gauge formulation has the following advantages: (a) The constraint is treated in a natural way—there is no explicit Lagrange multiplier—and (b) infrared divergences (which we discuss below) do not appear. However, the radial gauge suffers from the disadvantages that a functional integral formulation of the theory must be used and that the f' operators have no direct physical meaning.

In this paper we use the Cartesian gauge. It amounts to making a direct $1/N$ expansion of the model defined by (2.5) and (2.7). It suffers from two principle disadvantages: One must keep track explicitly of the Lagrange multiplier field λ , and also infrared divergent terms may appear at intermediate stages of computations. On the other hand, the Cartesian gauge permits a Hamiltonian approach; it also enables one to retain the physical electron operators c and f , and it provides a useful consistency check on calculations: The infrared divergences mentioned above and discussed further below must cancel in physical quantities. If they do not, either the computation is in error or one is calculating a physically meaningless quantity.

To generate a $1/N$ expansion we write^{14,2,3}

$$\tilde{A}_i^\dagger(t) = \frac{1}{\sqrt{N}} b_i^\dagger(t) , \quad (2.9a)$$

$$V = \sqrt{N} V_0 , \quad (2.9b)$$

$$1 = Q_i = q_0 N , \quad (2.9c)$$

and regard A and V as being of order 1. Our model is equivalent to the model defined by Eqs. (2.5) and (2.7) if $q_0 = 1/N$. However, to obtain a sensible $1/N$ expansion, we must formally treat q_0 as a parameter independent of the explicit factor of N , and only set $q_0 = 1/N$ at the end of a calculation. Note that it has been argued⁸ that the properties of, say, the spin- $\frac{1}{2}$ Anderson model are best represented by performing a $1/N$ expansion with $q_0 = \frac{1}{2}$. We do not adopt this view here. Rather, we expand any physical quantity $F(q_0)$ as

$$F(q_0) = F_0(q_0) + \frac{1}{N} F_1(q_0) + \cdots + \frac{1}{N^k} F_k(q_0) + \cdots ,$$

and then set $q_0 = 1/N$. This procedure is sensible as long as the $F_k(q_0 = 1/N)$ do not grow like N^k . We have no general proof that this is so, but results to be presented in subsequent sections provide an *a fortiori* justification for the assumption. We also note that the two small quantities, q_0 and $1/N$, play very different roles in the formal structure of the theory. $1/N$ controls the loop expansion in Bose fluctuations about the mean-field theory, whereas q_0 enters simply as a parameter, although we emphasize that the original model is regained only when $q_0 = 1/N$. Note also that the calculations simplify considerably in the small q_0 limit if we assume that the number of c electrons per spin channel is of order 1 and not of order $1/N$ or order q_0 . We make this assumption henceforth.

We now make the lattice analogue of the broken-symmetry ansatz of Read and Newns³ and Coleman.² This amounts to assuming that the ground state $|\varphi\rangle$ is such that

$$\langle \varphi | \tilde{A}_k | \varphi \rangle = a \delta_{k0} , \quad (2.10a)$$

$$\langle \varphi | \tilde{\lambda}_k | \varphi \rangle = (\varepsilon_f - E_0) \delta_{k0} , \quad (2.10b)$$

where a and $\varepsilon_f - E_0$ are constants to be determined. Then, shifting \tilde{A}_k and $\tilde{\lambda}_k$ so that

$$\tilde{A}_k = A_k + a\delta_{k0}, \quad (2.11a)$$

$$\tilde{\lambda}_k = \lambda_k + (\epsilon_f - E_0)\delta_{k0} \quad (2.11b)$$

(where $\langle \varphi | A_k | \varphi \rangle = \langle \varphi | \lambda_k | \varphi \rangle = \langle \varphi | A_k^\dagger A_k | \varphi \rangle = 0$), one may rewrite the Hamiltonian, Eqs. (2.5) and (2.7) as

$$H = H_0 + H_{\text{int}} + H_A, \quad (2.12)$$

where

$$H_0 = \sum_{k,m} \epsilon_k c_{km}^\dagger c_{km} + \epsilon_f f_{km}^\dagger f_{km} + Va(c_{km}^\dagger f_m + \text{H.c.}) + N \sum_k (\epsilon_f - E_0) A_k^\dagger A_k + Na \sum_k (A_k^\dagger + A_{-k}) \lambda_k, \quad (2.13a)$$

$$H_{\text{int}} = V \sum_{k,q,m} (c_k^\dagger f_{k+q} A_q^\dagger + \text{H.c.}) + \sum_{k,q} \lambda_q \left[NA_{k+q}^\dagger A_k + \sum_m f_{k+q}^\dagger m f_{km} \right], \quad (2.13b)$$

$$H_A = N(\epsilon_f - E_0)a(A_0^\dagger + A_0) + N(a^2 - q_0)\lambda_0. \quad (2.13c)$$

This Hamiltonian describes electrons moving in the band structure which is determined by H_0 and is shown in Fig. 1, and interacting with two sorts of bosons via H_{int} . The parameters a and ϵ_f are to be chosen so that H_A does not contribute to physical processes.¹⁴

Because the terms in H quadratic in boson fields are of order N , the boson propagators are of order $1/N$. Thus, an expansion in boson-fermion interactions is an expansion in $1/N$. Indeed, it will be seen that the simplifications resulting from an expansion in $1/N$ are very similar to those resulting from the smallness of m/M (m denotes

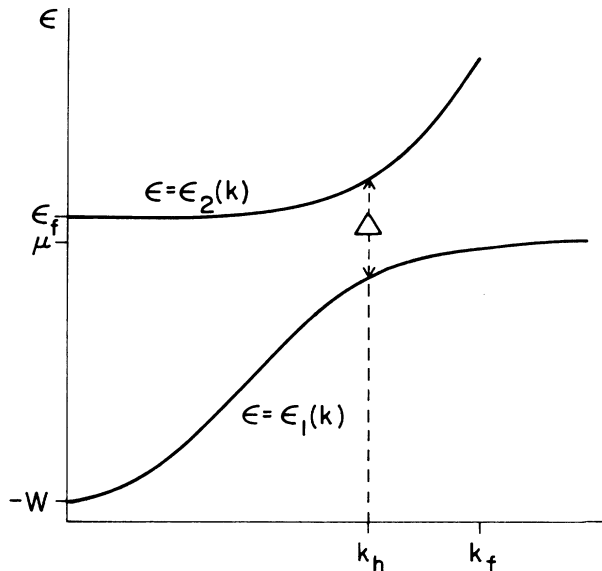


FIG. 1. Sketch of energy ϵ vs wave number k dispersion relation for the quasiparticle bands derived from H_0 . A less-than-half-filled band is assumed. Note the flatness of the lower band at $k = k_f$.

electron mass, M denotes ion mass) in the electron-phonon problem. Further, the parameter ϵ_f here plays the role of the Debye frequency ω_D in the phonon problem.

There are, however, several important differences between the electron-phonon problem and the electron-slave-boson problem we consider here. First, as will be shown in a subsequent section, the energy scale ϵ_f is also the Fermi energy characterizing the fermi-liquid ground state. In the electron-phonon problem, the Fermi energy is much larger than the Debye energy. Second, phonons of low energy necessarily have long wavelength. This is not true in the case at hand; rather, the boson propagator is only weakly dependent on wave vector. This difference arises because the boson field is essentially a bookkeeping device introduced to ensure that a *local* constraint [Eq. (2.1b)] is respected; there is therefore no physical reason for it to become soft as $q \rightarrow 0$.

We may, however, exploit the analogy with the electron-phonon problem as follows. First, provided perturbation theory is valid (i.e., provided that it does not predict a phase transition), the electron-boson interactions (as also the electron-phonon interactions) can have only two effects. One is to renormalize the numerical values of static quantities (in more elaborate language, to renormalize Landau parameters); within our model these changes will be of order $1/N$ and can lead to no qualitative changes in our results. Except in our computation of the Wilson ratio, such renormalizations will be ignored in this paper. One case is known in which a small interaction can lead to a dramatic change in the ground state: superconductivity. Just as the electron-phonon interaction leads to superconductivity, so can the electron boson interaction. This is treated in another paper.

Second, as will be shown below, the boson propagators vary with energy on a scale set by ϵ_f , but vary with wave vector only on a scale set by k_f . This leads to simplifications analogous to those arising in the electron-phonon problem.

We have argued (except for a superconducting instability) the effects of the electron-boson interaction may be neglected for static properties. As with the electron-phonon interaction, there are nontrivial frequency-dependent effects. These will be considered in Sec. V and in a subsequent paper.

As mentioned above, infrared divergences occur at intermediate stages of calculations in the Cartesian formulation used here. The meaning of the infrared divergences has been explained by Read¹⁵ in the context of the one-impurity problem. We will restate and extend Read's analysis here. The essential point is that in writing Eq. (2.11a) we have fixed the phase of the boson field at every lattice site. As is well known¹⁶ the phase of a quantum field is conjugate to the number operator for the field, in the same sense that position and momentum operators are conjugate in ordinary quantum mechanics. A state in which the boson field has a definite phase is accordingly a state in which the uncertainty in the expectation value of the boson number operator is infinite. If the uncertainty in the boson number operator is infinite, one cannot satisfy the constraint (2.4) on any lattice site. Indeed, since we

must have $n_f^i + n_b^i = 1$ at each site i , we must require that the uncertainty in n_b^i is less than 1. By the number-phase uncertainty relation, it follows that the uncertainty in the phase of the boson at any site is $> 2\pi$. We therefore conclude that (1) Eq. (2.11a), which ascribes a definite phase to the boson operator at each site, cannot hold in the true ground state, and (2) there can be no static phase correlation between any two different lattice states i and j .

The stronger conclusion (2) arises because we have a local constraint. It is worth contrasting this situation with the more familiar case of superconductivity. In this case, although one can work in a state of definite total number of particles, and therefore in a state in which the uncertainty in the phase of the superconducting order parameter is $> 2\pi$, there is no reason why the number of particles in one subsystem of the superconductor need be conserved, and therefore the phase at any arbitrary point in the superconductor is fixed when its value at any one point is known.

At any rate, in light of conduction (2) above, the boson fluctuations must act to restore the broken symmetry by forcing one to average over the phases at each lattice site independently. Indeed if one rewrites the boson operators A^\dagger, A as an amplitude

$$R(q, i\nu) = (1/\sqrt{2})[A^\dagger(q, i\nu) + A(-q, -i\nu)]$$

and phase

$$\theta(q, i\nu) = (1/\sqrt{2})[A^\dagger(q, i\nu) - A(-q, -i\nu)],$$

one finds that the phase-phase propagator diverges as $1/\nu^2$, while the amplitude-amplitude propagator does not diverge. Remarkably, as was first shown by Read¹⁵ for the single-impurity problem, and as we have verified in the lattice case, the infrared divergences cancel in physical quantities [to $O(1/N)$], leaving finite results. A good definition of "physical quantity" is "one whose computation does not violate the constraint, (2.4)." An example will make this clear.

To study the propagation of f electrons, one might be tempted to calculate the quantity $\langle T_\tau f_i(\tau) f_j^\dagger(\tau') \rangle$. One can compute it in a $1/N$ expansion in our model; it is infrared divergent at order $1/N$. The reason is that at time τ' one has added an f electron at site j . Thus from time τ' to time τ the system is in a state in which $n_f^j + n_b^j = 2$, violating the constraint (2.4). This leads to infrared divergences. The correct object to study is $\langle T_\tau b_i^\dagger(\tau) f_i(\tau) f_j^\dagger(\tau') b_j^\dagger(\tau') \rangle$. At no time in the calculation of this quantity is the constraint violated. We have shown that infrared divergences cancel in it.

In the remainder of this section we discuss the formal details of the $1/N$ expansion. We first derive some general properties of the mean-field Hamiltonian; then we obtain the leading order (in $1/N$) expressions for the mean-field parameters ε_f and a . Many of the details of the computation have been relegated to the Appendix.

We begin with the mean-field Hamiltonian H_0 , Eq. (2.13a). It is convenient to diagonalize the fermion part of H_0 and rewrite the c and f operators in terms of the operators d_1 and d_2 , which pertain to electrons in the lower and upper bands of Fig. 1, respectively. The relations are

$$d_{1km} = u_k f_{km} + v_k c_{km}, \quad (2.14a)$$

$$d_{2km} = -v_k f_{km} + u_k c_{km} \quad (2.14b)$$

with

$$u_k^2 = \frac{1}{2} \left[1 + \frac{\varepsilon_k - \varepsilon_f}{E_k} \right], \quad (2.15a)$$

$$v_k^2 = \frac{1}{2} \left[1 - \frac{\varepsilon_k - \varepsilon_f}{E_k} \right], \quad (2.15b)$$

and

$$E_k = [(\varepsilon_k - \varepsilon_f)^2 + 4(Va)^2]^{1/2}. \quad (2.15c)$$

One also finds

$$u_k^2 + v_k^2 = 1, \quad (2.16a)$$

$$u_k v_k = Va/E_k, \quad (2.16b)$$

and, further, that the energies of the lower (1) and upper (2) bands are

$$\varepsilon_1(k) = \frac{1}{2}(\varepsilon_k + \varepsilon_f - E_k), \quad (2.17a)$$

$$\varepsilon_2(k) = \frac{1}{2}(\varepsilon_k + \varepsilon_f + E_k). \quad (2.17b)$$

We must also fix the position of k_F . In the absence of a magnetic field, this is fixed by the total number of electrons, in accord with Luttinger's theorem.¹⁷ The argument is as follows.

The "spin" degeneracy is N ; if one assumes n electrons per site (counting both c and f) then two cases arise. If $n < N$, k_F is chosen so that the Fermi volume contains n electrons per site. If $N < n < 2N$, there is one filled band, and k_F is chosen so that the Fermi volume contains $n - N$ electrons per site. We assume always $n < N$. The results for $N < n < 2N$ are qualitatively similar.

Because our energies are measured relative to the chemical potential, we have $\varepsilon_1(k_F) = 0$ or, using Eqs. (2.2) and (2.17a),

$$k_F = k_h(1 + V^2 a^2 / \varepsilon_f W)^{1/2} = k_h[1 + O(q_0)]. \quad (2.18)$$

The last equality follows from the discussion after Eq. (2.9).

We define bare-fermion Green functions via

$$G_c^m(k, \tau) = \langle T_\tau c_{km}^\dagger(\tau) c_{km}^\dagger(0) \rangle_0, \quad (2.19a)$$

$$G_f^m(k, \tau) = \langle T_\tau f_{km}(\tau) f_{km}^\dagger(0) \rangle_0, \quad (2.19b)$$

$$G_m^m(k, \tau) = \langle T_\tau f_{km}(\tau) c_{km}^\dagger(0) \rangle_0. \quad (2.19c)$$

τ is an imaginary time, T_τ is the imaginary-time ordering operator, and $\langle \rangle_0$ denotes an expectation value in the system described by H_0 . Transforming to Matsubara frequencies, we find

$$\begin{aligned} G_c(k, i\omega) &= \frac{i\omega - \varepsilon_f}{(i\omega - \varepsilon_f)(i\omega - \varepsilon_k) - V^2 a^2} \\ &= \frac{v_k^2}{i\omega - \varepsilon_1(k)} + \frac{u_k^2}{i\omega - \varepsilon_2(k)}, \end{aligned} \quad (2.20a)$$

$$G_f(k, i\omega) = \frac{i\omega - \varepsilon_k}{(i\omega - \varepsilon_f)(i\omega - \varepsilon_k) - V^2 a^2} \\ = \frac{u_k^2}{i\omega - \varepsilon_1(k)} + \frac{v_k^2}{i\omega - \varepsilon_2(k)}, \quad (2.20b)$$

$$G_m(k, i\omega) = \frac{Va}{(i\omega - \varepsilon_f)(i\omega - \varepsilon_k) - V^2 a^2} \\ = \frac{-Va/E_k}{i\omega - \varepsilon_1(k)} + \frac{Va/E_k}{i\omega - \varepsilon_2(k)}. \quad (2.20c)$$

We also define bare boson propagators. We defer discussion of the λ field. Because of the broken symmetry, there are four propagators involving the A field. They are conveniently represented by a matrix D_0 , defined via

$$D_0(k, \tau) = \begin{pmatrix} \langle T_\tau A_k^\dagger(\tau) A_k(0) \rangle_0 & \langle T_\tau A_k^\dagger(\tau) A_{-k}^\dagger(0) \rangle_0 \\ \langle T_\tau A_{-k}(\tau) A_k(0) \rangle_0 & \langle T_\tau A_k(\tau) A_k^\dagger(0) \rangle_0 \end{pmatrix}. \quad (2.21a)$$

We have

$$D_0(k, \nu) = \frac{1}{N(\varepsilon_f - E_0)} \begin{pmatrix} 1 & 0 \\ 0 & 1 \end{pmatrix}. \quad (2.21b)$$

The fermions and bosons interact via the terms in H_{int} . We show the various possible interaction terms in Feynman graph notation in Fig. 2.

We now compute the mean-field parameters ε_f and a . They are determined as follows: the terms in H_A [Eq. (2.13c)] as well as those in H_I (2.13b) lead to “tadpole” graphs; ε_f and a are to be chosen so that these vanish. To leading order in N , the relevant tadpoles are those shown in Figs. 3(a) and 3(b). Requiring that these graphs sum to zero leads to

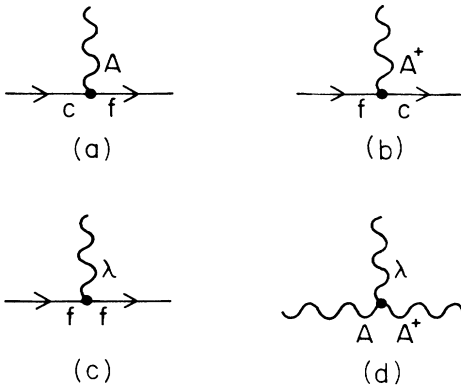


FIG. 2. Interaction terms arising from H_{int} , Eq. (2.13c). The wiggly line denotes a boson propagator (the boson operator that occurs at the vertex is explicitly indicated); the solid line with an arrow denotes a fermion propagator (the electron operators that occur at the vertex are also explicitly indicated).

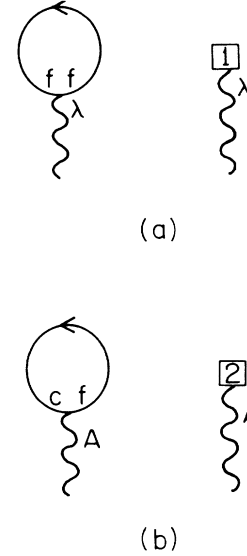


FIG. 3. Tadpole graphs to leading order in N . Requiring that these sum to zero fixes the parameters ε_f and a to leading order in N . In Fig. 2(a) the wiggly line represents a λ propagator at zero frequency and momentum. In Fig. 2(b) the wiggly line represents an A propagator at zero frequency and momentum. The boxes containing the numerals 1 and 2 arise from Eq. (2.13c).

$$N(a^2 - q_0) + \sum_{k, i\omega, m} G_f^m(k, i\omega) = 0, \quad (2.22a)$$

$$N(\varepsilon_f - E_0)a + \sum_{k, i\omega, m} G_m^m(k, i\omega) = 0. \quad (2.22b)$$

Equations (2.22) may be solved. The calculations are particularly simple in the Kondo limit, where Va and ε_f are much smaller than W , so that one may make the approximations listed in Eq. (A20). Consider first Eq. (2.22a). Using Eqs. (A17) and (2.20b), we find

$$a^2 = q_0 - \frac{1}{6\pi^2} (k_F^3 - k_h^3)$$

or, using Eq. (2.18), and rearranging,

$$a^2 = q_0 (1 - n_f) (1 - \frac{1}{4} n_f \alpha). \quad (2.23a)$$

Here $n_f = (1 + \varepsilon_f / \rho_0 V^2)^{-1}$ is the mean-field number of f electrons (to leading order in q_0) and $\alpha = q_0 n_f / \rho_0 W$.

Proceeding similarly with Eq. (2.22b), we find that the dominant term in the sum on k, ω is a logarithm. To leading logarithmic accuracy one finds

$$\varepsilon_f - E_0 = \rho_0 V^2 \ln \left[\frac{4W^2}{V^2 a^2} \right] \left[\frac{k_F - k_h}{k_F + k_h} \right],$$

or using Eq. (2.18), $\varepsilon_f / \rho_0 V^2 \ll 1$, and rearranging,

$$\varepsilon_f = W \left[1 - \frac{q_0}{\rho_0 W} \right] \exp(E_0 / \rho_0 V^2). \quad (2.23b)$$

Note that to leading order in q_0 and N , ε_f is given by the usual leading order (in N) expression for the single-

impurity Kondo temperature. ϵ_f is of order $(1/N)^0 \sim 1$.

Substitution of the results for ϵ_f and a shows that the bands are very flat near the Fermi surface, with an effective mass m^* related in the Kondo limit to the usual electron mass m via

$$\frac{m^*}{m} = \frac{V^2 a^2}{\epsilon_f^2} = \frac{\epsilon_{k_F}^2}{V^2 a^2}. \quad (2.24)$$

Although the mass enhancement is order q_0 and by Eq. (2.9c) $q_0 = 1/N$, the mass enhancement is still very large. For a typical system one might have $\epsilon_f \sim 1-10$ meV,

while $W \sim 1$ eV.

We now compute the leading-order dressed boson propagators from the usual Dyson equation:

$$D^{-1}(q, \nu) = D_0^{-1}(q, \nu) - \Sigma(q, \nu). \quad (2.25)$$

Because, by Eq. (2.22), $D_0^{-1} \sim N$, we need only consider order N contributions to Σ . The only such term is a fermion bubble, which has a factor of N from the spin sum. The relevant fermion bubbles are shown in Fig. 4. The diagrams are evaluated in the Appendix. The result is

$$D^{-1}(q, i\nu) = \begin{pmatrix} i\nu[1 - P_1(q, i\nu)] + P_M(q, i\nu) & P_m(q, \nu) \\ P_m(-q, -i\nu) & -i\nu[1 - P_1(-q, -i\nu)] - P_m(q, i\nu) \end{pmatrix} \quad (2.26)$$

and

$$\det D^{-1}(q, i\nu) = \nu^2 \{ [1 - P_1(q, i\nu)][1 - P_1(-q, -i\nu)] + P_M(q, i\nu)P_f(q, i\nu)/V^2 a^2 \}. \quad (2.27)$$

$$\Sigma_{A^+A}(k, i\nu) = \begin{array}{c} \text{p+k, } i\omega+i\nu \\ \text{c} \quad \text{c} \\ \text{f} \quad \text{f} \\ \text{p, } i\omega \end{array}$$

$$\Sigma_{AA}(k, i\nu) = \begin{array}{c} \text{p+k, } i\omega+i\nu \\ \text{f} \quad \text{c} \\ \text{c} \quad \text{f} \\ \text{p, } i\omega \end{array}$$

$$\Sigma_{A^+A^+}(k, i\nu) = \begin{array}{c} \text{p+k, } i\omega+i\nu \\ \text{c} \quad \text{f} \\ \text{f} \quad \text{c} \\ \text{p, } i\omega \end{array}$$

$$\Sigma_{AA^+}(k, i\nu) = \begin{array}{c} \text{p+k, } i\omega+i\nu \\ \text{f} \quad \text{f} \\ \text{c} \quad \text{c} \\ \text{p, } i\omega \end{array}$$

FIG. 4. Matrix of self-energies for finite-frequency boson propagator.

The various polarization bubbles are defined by

$$P_1(q, i\nu) = \frac{-V}{a} \sum_{p, \omega} G_f(p, \omega) G_M(p+q, \omega+\nu), \quad (2.28a)$$

$$P_M(q, i\nu) = V^2 \sum_{p, \omega} G_M(p, \omega) G_m(p+q, \omega+\nu), \quad (2.28b)$$

$$P_f(q, i\nu) = V^2 \sum_{p, \omega} G_f(p, \omega) G_f(p+q, \omega+\nu). \quad (2.28c)$$

Note that the off-diagonal terms in Eq. (2.26) contain a factor of a^2 in the numerator relative to the diagonal terms. The off-diagonal terms are therefore of order $1/N$ relative to the diagonal terms; however, the diagonal terms tend to zero as $i\nu \rightarrow 0$, so the off-diagonal terms may not simply be dropped.

Note that because we have been restricted to $i\nu \neq 0$, any infrared divergences will be cut off by thermal effects for temperature $T \neq 0$. However, we shall show below and in subsequent sections that even at $T=0$, infrared divergences cancel in all physical quantities.

We now consider the special case $i\nu=0$. The λ field enters here; this ensures that the system is in the correct ground state. The λ field mixes with the field $R_k = 1/\sqrt{2}(A_k^\dagger + A_{-k})$, but as may easily be shown from (2.13a) and (2.26), R_k is the only combination of A fields present at $i\nu=0$. The self-energies for this case are shown in Fig. 5. Defining a new zero-frequency bose propagator \tilde{D} by

$$\tilde{D}(q) = \begin{pmatrix} \langle R_k R_{-k} \rangle & \langle R_k \lambda_{-k} \rangle \\ \langle \lambda_k R_{-k} \rangle & \langle \lambda_k \lambda_{-k} \rangle \end{pmatrix}, \quad (2.29)$$

we find at zero frequency

$$\tilde{D}^{-1}(q) = \begin{pmatrix} P_M(q, 0) & a[1 - P_1(q, 0)] \\ a[1 - P_1(q, 0)] & P_f(q, 0)/V^2 \end{pmatrix}. \quad (2.30)$$

$$\Sigma_{RR}(k) = \frac{1}{2} \left[\begin{array}{c} \text{c} \rightarrow \text{c} \\ \text{f} \leftarrow \text{f} \end{array} \oplus \begin{array}{c} \text{f} \rightarrow \text{f} \\ \text{c} \leftarrow \text{c} \end{array} \oplus \begin{array}{c} \text{c} \rightarrow \text{f} \\ \text{f} \leftarrow \text{c} \end{array} \oplus \begin{array}{c} \text{f} \rightarrow \text{c} \\ \text{c} \leftarrow \text{f} \end{array} \right]$$

$$\Sigma_{R\lambda}(k) = \frac{1}{2} \left[\begin{array}{c} \text{c} \rightarrow \text{f} \\ \text{f} \leftarrow \text{f} \end{array} \oplus \begin{array}{c} \text{f} \rightarrow \text{f} \\ \text{c} \leftarrow \text{f} \end{array} \right]$$

$$\Sigma_{\lambda R}(k) = \Sigma_{R\lambda}(k)$$

$$\Sigma_{\lambda\lambda}(k) = \frac{1}{2} \left[\begin{array}{c} \text{f} \rightarrow \text{f} \\ \text{f} \leftarrow \text{f} \end{array} \right]$$

FIG. 5. Matrix of self-energies for zero-frequency boson propagator. Assignment of momenta to Fermi loops is as in Fig. 4.

We now complete the formal development by considering the $1/N$ corrections to the mean-field parameters ϵ_f and a . The relevant diagrams are shown in Fig. 6. The resulting equations are complicated, but the infrared divergent parts are easily extracted. Writing $a = a_0 + (1/N)a_1$ and $\epsilon_f = \epsilon_{f0} + (1/N)\epsilon_{f1}$, with a_0 and ϵ_{f0} given by Eq. (2.21a) and (2.21b), we find that ϵ_{f1} is not infrared divergent, but that the divergent part of a_1, a_1^* is given by

$$a_1^* = \frac{N}{a_0} \sum_{k, i\nu \neq 0} \frac{2P_M(k, i\nu)}{\det D^{-1}(k, i\nu)}. \quad (2.31)$$

As in the single-impurity problem,¹⁵ divergences due to the boson propagators cancel the divergences caused by the shift in the parameter a , leaving physical quantities finite.

We conclude the section by showing that

$$\langle Q_i(\tau) - 1 \rangle = 0, \quad (2.32a)$$

$$\langle T_\tau [Q_i(\tau) - 1][Q_j(0) - 1] \rangle = \chi_Q(i, j; \tau) = 0. \quad (2.32b)$$

These results provide strong evidence that the constraint, Eq. (2.4), is enforced by our formalism.

To see this, pick a site, say site j , and expand the ground state of our model in a basis of states with definite values of Q_j : $|\varphi\rangle = \sum_{n \geq 0} |\varphi_n\rangle$ with $Q_j |\varphi_n\rangle = n |\varphi_n\rangle$ [Eq. (2.8) shows that this is possible; the usual derivation

$$\chi_Q(i, j; \tau) < T_\tau \left[Na [a_i^\dagger(\tau) + A_i(\tau)] + \sum_m f_{im}^\dagger(\tau) f_{im}(\tau) \right] \left[Na [A_j^\dagger(0) + A_j(0)] + \sum_m f_{jm}^\dagger(0) f_{jm}(0) \right].$$

The order- N diagrams corresponding to this expression are shown in Fig. 7. They are most conveniently evaluated in k, ν space. We consider first $\nu \neq 0$. The λ field then does not enter, and

$$\chi_Q(k, i\nu) = \frac{N}{\nu^2} P_f(k, i\nu) + \frac{1}{2} \text{Tr} M(k, i\nu) D(k, i\nu) M(-k, -i\nu), \quad (2.34)$$

where D is given by

$$M(k, i\nu) = Na \begin{bmatrix} 1 - P_1(k, i\nu) & 1 - P_1(-k, -i\nu) \\ 1 - P_1(-k, -i\nu) & 1 - P_1(+k, +i\nu) \end{bmatrix}. \quad (2.35)$$

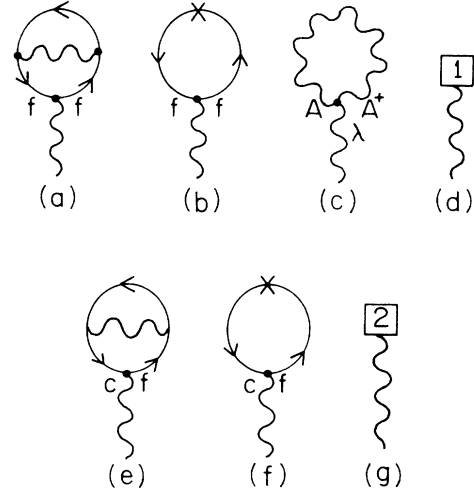


FIG. 6. Tadpole diagrams to order $1/N$. The notation is as in Fig. 2. In (a) and (e) the wiggly line running across the Fermi loop represents the matrix of A propagators (if the frequency across the wiggly line is not zero) or the matrix of $R\lambda$ propagators (if the frequency across the wiggly line is zero). In (c) the boson operator that corresponds to the wiggly line has been explicitly indicated. The symbol \times which occurs in (b) and (f) (which are diagrams that appeared in Fig. 2) means that one should substitute $a \rightarrow a_0 + (1/N)a_1$ and $\epsilon_f \rightarrow \epsilon_{f0} + (1/N)\epsilon_{f1}$ in the expressions derived from the diagrams in Fig. 2 and expand to order $1/N$.

of second quantization shows that Q_j has the discrete spectrum given]. Thus Eq. (2.32a) shows that $\sum_n (n |a_n|^2) = \sum_n |a_n|^2$, but (2.32b) shows $\sum_n (n-1)^2 |a_n|^2 = 0$, which can only be satisfied if $a_n = 0$ unless $n=1$. Note also that by Eq. (2.8), the dynamics generated by H conserve the value of Q_j ; thus as long as we do not try to compute operators which do not commute with Q_j , the crucial constraint, Eq. (2.4), is preserved by our model.

We now write

$$Q_i = N(a + A_i^\dagger)(a + A_i) + \sum_m f_{im}^\dagger f_{im}. \quad (2.33)$$

Then using the expressions given after (2.11b) and also Eq. (2.23a), we may easily establish (2.32a). Setting (2.33) into (2.32b) and using (2.32a) then leads to

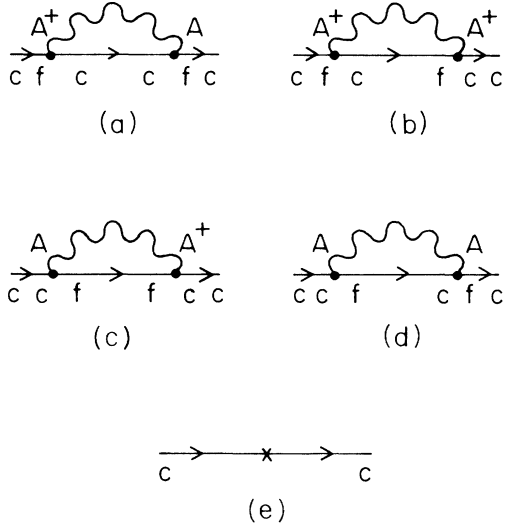


FIG. 7. Self-energy corrections to c -electron Green functions. The notation \times is as in Fig. 6. There should also be diagrams involving the λ field. These are not infrared divergent; and they do not contribute to the imaginary part of the self-energy. They have therefore not been explicitly written.

Performing the trace and using identities given in the Appendix immediately yields the desired result. Now consider the case $i\nu=0$. The λ field enters here; one may think of it as projecting out of the “mean-field” ground state of H_0 [Eq. (2.13a)] any components with quantum numbers $\langle Q_j \rangle \neq 1$. In this case the expressions are slightly different, because it is convenient to use the Bose field $R = (1/\sqrt{2})(A^\dagger + A)$. One obtains

$$\chi_Q(k, iN=0) = \frac{1}{V^2} P_f(k, i\nu=0) + \frac{1}{2} \text{Tr} M_1(k) D(k) M_1(k),$$

where now $D(k)$ is given by (2.27) and

$$M_1(k) = Na \begin{bmatrix} 1 - P_1(k, 0) & 1 - P_1(k, 0) \\ -P_f(k, 0) & -P_f(k, 0) \end{bmatrix}.$$

Again, performing the trace one obtains $\chi_Q(k, 0) = 0$.

III. THERMODYNAMICS

In this section we consider the thermodynamics of our model to leading and next-to-leading order in $1/N$. We show that the specific heat $C = \gamma T$ and susceptibility χ are finite to order $1/N$. We explicitly compute the Wilson ratio $R = \chi/\gamma$ to order $1/N$. R is interesting because its divergence signals a ferromagnetic instability. It has been argued that the Anderson lattice in the Kondo limit will be unstable towards some form of magnetic order, except in a large- N limit. A criterion for stability which has appeared in the literature is^{9,18}

$$N > |E_0|/\Delta_0. \quad (3.1)$$

We have rewritten the result in our notation. We may use Eqs. (2.23b) and (2.24) to write $|E_0|/\Delta_0$

$\sim \ln(Nm^*/m)$. Thus, with this view, the larger the mass enhancement, the greater the tendency toward magnetism. For, say, $m^*/m \sim 200$, one must have $N > 7$ for stability.

In contrast, we find within our $1/N$ expansion a much less stringent condition,

$$N > 1, \quad (3.2)$$

indicating that the Kondo lattice is much less unstable towards magnetic order than previously believed. Of course, our spin- N conduction band is not realistic, therefore (3.2) cannot be applied directly to real systems. Here we merely stress that to order $1/N$ we find no relation between mass enhancement and tendency towards magnetic instability.

We now turn to our computation. We shall obtain γ , χ , and R by computing the free energy F and differentiating with respect to temperature T and magnetic field h . The dependence of F on T is easy to compute within the Matsubara formalism we use. The dependence of F on h for a realistic Anderson lattice would be very complicated, for reasons analogous to those discussed in Sec. II in the context of our choice of a $1/N$ expansion. Therefore, in the spirit of our earlier approximations we may couple h to the bare Hamiltonian (2.5) via [the factor N is inserted so that χ is $O(N)$]

$$\varepsilon_k \rightarrow \varepsilon_{km} = \varepsilon_k + hm/N,$$

$$E_0 \rightarrow E_{0m} = E_0 + hm/N.$$

Retracing the steps that led to Eqs. (2.13) shows that we couple the field to the final Hamiltonian Eqs. (2.13) via

$$\varepsilon_k \rightarrow \varepsilon_{km} = \varepsilon_k + hm/N, \quad (3.3a)$$

$$\varepsilon_{f0} \rightarrow \varepsilon_{fm} = \varepsilon_f + hm/N. \quad (3.3b)$$

Note that R is relatively easy to compute within a $1/N$ expansion,¹⁵ for if one has

$$\gamma = \gamma_N(1 + a/N),$$

$$\chi = \chi_N(1 + b/N),$$

then

$$R = (\gamma_N/\chi_N)[1 + (b-a)/N]. \quad (3.4)$$

We now compute F . The leading order contribution F_0 has no boson lines and may be written

$$F_0 = \sum_{k, \omega, m} \ln G_{1m}(k, i\omega) + \ln G_{2m}(k, i\omega), \quad (3.5)$$

where

$$G_{1(2)m} = \frac{1}{i\omega - \varepsilon_{1,2}^m(k)}. \quad (3.6)$$

Here G_1 (G_2) is the Green function appropriate to the lower (upper) band of H_0 [Eq. (2.15a)]. F_0 may be differentiated in the usual way; one finds

$$\gamma = (m^*/m)\gamma_0 = \frac{Nm^*k_F}{6}, \quad (3.7a)$$

$$\chi = (m^*/m)\chi_0 = \frac{Nm^*k_F}{18}, \quad (3.7b)$$

$$R = 1. \quad (3.7c)$$

m^*/m was defined in Eqs. (2.24); γ_0 and χ_0 are the specific-heat coefficient and susceptibility that a noninteracting band of c electrons filled to $k=k_F$ would have. It is instructive to use the expressions for m^*/m and a^2 derived in Sec. II to write

$$\gamma = \frac{\pi^3}{3} \frac{n_f}{\varepsilon_f} (1 + \alpha/4). \quad (3.8)$$

In the limit $\alpha=0$, this is precisely the leading order one-impurity result¹⁵ (note γ is normalized to the unit cell). The order α corrections are due to lattice effects, in agreement with the ideas of Read and Newns.³

We now consider F_1 , the $1/N$ correction to F . As in the single-impurity calculation,¹⁵ there are two contributions to F_1 : one is shown by the diagrams in Fig. 8; the other arises from setting the $1/N$ corrections to the parameters ε_f and a into the leading order expression F_0 and expanding to order $1/N$. These latter contributions give identical contributions to χ and γ , up to trivial factors, and therefore do not contribute to R ; they do, however, lead to infrared divergent terms γ_1^*, χ_1^* in the $1/N$ corrections to γ and χ . One finds, e.g.,

$$\gamma_1^* = (1/N)(a_1^*/a_0)\gamma_0. \quad (3.9)$$

Now consider the contribution, F_1^B , to F_1 from the diagrams shown in Fig. 8. These may be summed; one finds

$$F_1^B = - \sum_{k, i\nu \neq 0} \ln \det \underline{D}^{-1}(k, i\nu). \quad (3.10)$$

F_1^B depends on temperature through the sum on the Matsubara frequency ν . It also depends on h and T through the fermion bubbles which make up D^{-1} . This latter dependence is the same, up to trivial factors, for T and h , and therefore does not contribute to R ; it does, however, lead to infrared divergent contributions γ_B^* and χ_B^* to γ and χ . We find, e.g.,

$$\gamma_B^* = - \sum_{k, i\nu \neq 0} \text{Tr} \left[\underline{D}(k, i\nu) \frac{\partial^2}{\partial T^2} \underline{D}^{-1}(k, i\nu) \right]. \quad (3.11)$$

After converting the frequency sum to a contour integral in the usual way, one may easily verify that the only infrared divergent term in (3.10) comes from differentiating the term that cancels the bare-boson energy ($\varepsilon_f - E_0$). Application of Eqs. (A.9) and (2.31) shows that the infrared divergences arising from Eqs. (3.9) and (3.11) sum to zero, so that the $1/N$ corrections to γ and, similarly, χ cancel, as they must.

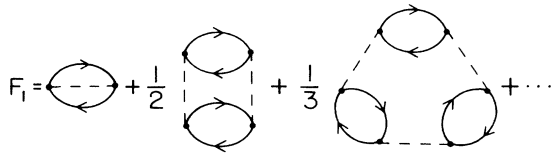


FIG. 8. Diagrams for the free energy. The light line is the bare-boson propagator, which must be used to avoid double counting. Diagrams involving λ lines may be omitted for reasons explained in the text.

We now compute R . The only term that contributes to the temperature dependence, but not the field dependence, of F_1 comes from the temperature dependence implicit in the frequency sum. This sum is evaluated by converting it to a contour integral and wrapping the contour around the real axis in the usual way, leading to

$$F_1^B = - \sum_k \int \frac{d\varepsilon}{\pi} n_B(\varepsilon) \tan^{-1} \frac{\text{Im} \det D^{-1}(q, \varepsilon + i\delta)}{\text{Re} \det D^{-1}(q, \varepsilon)}. \quad (3.12)$$

Here $n_B(\varepsilon)$ is the usual Bose function:

$$n_B(\varepsilon) = \frac{1}{e^{\beta\varepsilon} - 1}. \quad (3.13a)$$

As $T \rightarrow 0$ we have

$$n_B(\varepsilon) = -\Theta(-\varepsilon) + \frac{\pi^2}{3} k_B^2 T^2 \delta'(\varepsilon). \quad (3.13b)$$

Here $\delta'(\varepsilon)$ is the derivative of the dirac δ function.

Further, as shown in Appendix A, one finds that as $\varepsilon \rightarrow 0$, $\text{Im}[\det D^{-1}(q, \varepsilon + i\delta)] \rightarrow \varepsilon^3$, while $\text{Re}[\det D^{-1}(q, \varepsilon + i\delta)] \rightarrow \varepsilon^2$. The T^2 part of F_1 may therefore be easily extracted, and so one finds for R_1 , the $1/N$ correction to R :

$$R_1 = - \frac{1}{N\gamma_0} \frac{m^* k_F}{2\pi^2} \lim_{\varepsilon \rightarrow 0} \sum_q \frac{\text{Im} \det D^{-1}(q, \varepsilon + i\delta)}{\varepsilon \text{Re} \det D^{-1}(q, \varepsilon)}. \quad (3.14)$$

Using Eqs. (A.21) and (A.22) and working to leading order in α , we find

$$R_1 = \alpha k_f^3 [1 - (1 - n_f)^2] / 8\pi^2 \varepsilon_f \gamma_0 = [1 - (1 - n_f)^2] / N. \quad (3.15)$$

This result has been previously obtained by Read in the context of the single-impurity problem.¹⁵ We note that this result is consistent with the ansatz

$$R = \frac{1}{1 - a/N}, \quad (3.16)$$

where $a = 1 - (1 - n_f)^2$. In the Kondo limit of primary interest here, $a \sim 1$. This justifies the instability criterion (3.2).

One may also expand (3.14) to next order in α , obtaining a contribution to R of order q_0/N . We note that this contribution is "nonuniversal:" It depends, through α , on the density of electrons n , and, through the logarithm, on k_F . Both n and k_F may vary from material to material. Formally, we have no right to retain this term, because it is of order $1/N^2$, and there are other $1/N^2$ terms we have not computed. Nevertheless, we write it down for completeness:

$$R_2 = 0.07 q_0 / N. \quad (3.17)$$

This result has been previously obtained by Auerbach and Levin.⁸

We now comment briefly on the result Eq. (3.16). First it (and results for specific heat and susceptibility, which we have not written down here), shows that we have gen-

erated a systematic $1/N$ expansion; this provides a test of the validity of our method of expansion and resolves the question raised in the discussion of Eq. (2.22). Second, our result for R seems not to be universal: Unlike the single-impurity result, the $1/N^2$ terms may vary from material to material. However, this nonuniversal quantity R is, in our expansion, still of order 1, and in particular does not depend on the parameter $|E_0|/\Delta_0$ to leading order in $1/N$ and q_0/N .

Finally, we comment on the difference between our criterion [Eq. (3.2)] for when the nonmagnetic ground state is favored over a magnetically ordered ground state, and the previously derived one [Eq. (3.1)]. Equation (3.1) has been derived in two ways: by comparing the one-impurity Kondo temperature with an estimate for a magnetic ordering temperature T_m due to the conventional Ruderman-Kittel-Kasuya-Yosida (RKKY) interaction [the strength of which may be estimated from the Anderson Hamiltonian, Eq. (2.1)], and via an explicit computation of R using the Gutzwiller method. It has been argued⁷ that the RKKY interaction is smaller by a factor of N in our model than it is in the simple estimate from Eq. (2.1); therefore, the comparison between ε_f and T_m does not apply to our model. The Gutzwiller calculation is difficult to compare directly with our treatment because in Ref. 9 a distinction was made between spin and orbital angular momentum of the f electrons. The magnetic field was coupled only to the spin, while the large- N limit was taken by increasing the orbital degeneracy.

IV. NATURE OF THE GROUND STATE

In this section we discuss the nature of the ground state derived in Sec. II. This ground state is nonmagnetic and, as shown in Sec. III, behaves thermodynamically like a Fermi liquid with a very large mass m^* . But according to one way of looking at the problem,⁵ a nonmagnetic ground state should not exist in the Kondo limit [Eqs. (2.3)] in which m^*/m is large. In this section we outline this argument and then show how our results resolve the problem. We also clarify the nature of the quasiparticle states of the Fermi liquid and discuss which physical quantities involve the enhanced effective mass and which do not.

We have argued in the beginning of Sec. II that in the Kondo limit of our model the f -electron sites are essentially singly occupied. In this limit one might expect each f site to have an electron of definite spin, and one might also expect these spins to order magnetically. The Kondo effect is usually invoked to explain why the spins do not order magnetically. The Kondo effect involves one magnetic impurity in a nonmagnetic metallic host. At low temperatures the interaction between the spin on the impurity and the conduction electrons leads to strong spin-flip scattering of those conduction electrons within an energy, T_K , of the Fermi surface. T_K is the Kondo temperature and is the single impurity analogue of our energy scale ε_f . In the large- N limit, both are given by the same formula, Eq. (2.20b). The strong interaction between the conduction electrons and the impurity spin leads, it has been argued,⁵ to the formation of a spin-polarization

cloud which contains one conduction electron and surrounds the impurity. The spin of the polarization cloud and the spin of the impurity lock together to form a singlet, so that the ground state is nonmagnetic. Since the energy scale of the problem is T_K , the cloud must be made up of electrons within an energy T_K of the Fermi surface, and must have a linear dimension $\xi_0 \sim v_F/T_K$.

One would like to extend this picture to a lattice, to describe the heavy-fermion materials. Two problems, however, immediately arise. One is that the distance ξ_0 is much greater than the inter- f -site spacing: the spin polarization clouds would therefore interfere with each other. Now it has been argued¹¹ that in the lattice case the appropriate length is $\xi_0^* = v_f^*/T_K$, where $v_f^* = (m/m^*)v_f$. Since one has, approximately,

$$m/m^* \sim T_K/W, \quad (4.1)$$

where W is the bandwidth, one would estimate

$$\xi_0^* \sim v_f^*/T_K \sim v_F/W \sim (1 \text{ lattice constant}). \quad (4.2)$$

If this were correct, the ‘‘interference’’ problem would disappear.

However, there is a more fundamental problem with this picture of a Kondo lattice:⁵ the spin polarization cloud is supposed to be a wave packet containing one electron, made up from electrons within T_K of the Fermi surface. But the total number of electrons available within T_K of the Fermi surface is $\sim T_K/W$. This is much less than one per site: there are not enough electrons available to compensate every spin.

We are therefore motivated to consider, within our model, how the c electrons are scattered near the Fermi surface and how the f spins are compensated, so that the ground state is nonmagnetic. We consider first the electron Green functions. We begin with the bare-fermion Green functions appropriate to H_0 . These are defined in Eqs. (2.19) and (2.20). We note from Eqs. (2.20) that near the Fermi surface the dispersion relation is $\omega = \varepsilon_1(k)$, but $\partial\varepsilon_1/\partial k = (m/m^*)v_f^0$ where v_f^0 is the bare c -electron velocity. The low-energy excitations of H_0 are therefore heavy fermions. However, G_f and G_M are unphysical: if one writes, i.e., G_f in spectral representation,

$$G_f = \sum_n \frac{\langle \varphi | f_{km} | n \rangle \langle n | f_{km}^\dagger | \varphi \rangle}{i\omega - E_n},$$

the eigenstates $|n\rangle$ obviously do not satisfy $Q_i |n\rangle = |n\rangle$ (because $Q_i |\varphi\rangle = |\varphi\rangle$ and we have added one f electron to go from $|\varphi\rangle$ to $|n\rangle$). Thus to compute G_f and G_M one must go outside the physical space defined by Eq. (2.4). Thus G_f and G_M must be viewed as convenient objects with which one may calculate physical quantities. They have no simple physical interpretation. G_C , on the other hand, does not suffer from this defect. We now interpret it physically. To do this it is useful to analytically continue it to real frequencies and to rewrite it as

$$G_C(k, \omega) = \frac{1}{\omega - \varepsilon_k - V^2 a^2 / (\omega - \varepsilon_f)}. \quad (4.3)$$

Consider low frequencies, $\omega \ll \varepsilon_f$ and wave vectors near k_f . Note $\varepsilon_{k_f} = V^2 a^2 / \varepsilon_f$. Then G_C may be approximately rewritten

$$G_C(k, \omega) = \frac{Z}{\omega - v_F^* |k - k_f|}, \quad (4.4)$$

where

$$Z = (1 + m^*/m)^{-1}. \quad (4.5)$$

Thus, near the Fermi surface the c electrons behave as quasiparticles of spectral weight $Z \ll 1$. In subsequent sections we show that this has interesting consequences for NMR relaxation and for the conductivity $\sigma(\omega, T)$.

Next, consider large frequencies, $\omega \gg Va$; then

$$G_C(k, \omega) = \frac{1}{\omega - \varepsilon_k}, \quad (4.6)$$

i.e., the c -electron Green function reverts to the form it

would have in the absence of hybridization. For frequencies of order Va and smaller, G_c is strongly modified. Note that in the one-impurity problem, c -electron propagation is only modified for energies of order $\varepsilon_f \sim (m/m^*)^{1/2} Va$ from the Fermi surface.

Finally, we compute the c -electron density of states, $\rho_c(\omega) = \sum \text{Im} G_c(k, \omega)$. Inspection of (4.3) shows $\rho_c(\omega) = \rho_0(\omega) = (dk/d\varepsilon_k)$, unless ω is in the gap in the band structure shown in Fig. 1. Thus, the c -electron density of states is essentially unenhanced. Another way of stating this result is that the quasiparticle density-of-states enhancement ($m^*/m \sim Z^{-1}$) cancels the quasiparticle spectral weight, to leading order in N .

We now consider the $1/N$ corrections to G_c . We show infrared divergences cancel in it and we compute $\text{Im} G_c$, which will be useful in our discussion of the conductivity, and, we will argue, may be measured in a tunneling experiment. The relevant diagrams are shown in Fig. 8. The analytic expression corresponding to these diagrams is

$$G_M(k, i\omega)^2 \sum_{q, i\nu} D_{11}(q, i\nu) G_C[k+q, i(\omega+\nu)] + 2G_M(k, i\omega) G_C(k, i\omega) \sum_{q, iN} D_{12}(q, i\nu) G_M[k+q, i(\omega+\nu)] \\ + G_c(k, i\omega)^2 \sum_{q, iN} D_{22}(q, i\nu) G_f[k+q, i(\omega+\nu)] + 2a_1 \frac{\partial}{\partial a_1} G_C(k, i\omega), \quad (4.7)$$

where

$$D_{11}(q, i\nu) = \{i\nu[1 - P_1(-q, -i\nu)] + P_m(q, i\nu)\} / \det D^{-1}(q, i\nu), \quad (4.8a)$$

$$D_{12}(q, i\nu) = [-P_m(q, i\nu)] / \det D^{-1}(q, i\nu), \quad (4.8b)$$

$$D_{22}(q, i\nu) = D_{11}(-q, -i\nu) \quad (4.8c)$$

(there are additional terms at $\nu=0$ which contribute neither to the infrared divergences nor to the imaginary part), $\det D^{-1}$ is given by Eq. (2.26). Because $\det D^{-1}$ is proportional to ν^2 the terms involving the D 's are infrared divergent.

We now write out explicitly the terms involving D in Eq. (4.7). All of these terms share the common factor

$$\sum_{q, i\nu} \frac{1}{[i\omega - \varepsilon_1(k)]^2 [i\omega - \varepsilon_2(k)]^2 \det D^{-1}(q, i\nu) [i(\omega+\nu) - \varepsilon_1(k+q)] [i\omega + \nu - \varepsilon_2(k+q)]}.$$

Suppressing this for the moment and using Eqs. (2.20), we find for the terms involving D in Eq. (4.7):

$$V^2 a^2 [i(\omega+\nu) - \varepsilon_f] \{-i\nu[1 - P_1(-q, -\nu)] + P_m(q, \nu)\} - 2V^2 a^2 (i\omega - \varepsilon_f) P_m(q, i\nu) \\ + (i\omega - \varepsilon_f)^2 [i(\omega+\nu) - \varepsilon_{k+q}] [i\nu - P_1(q, i\nu) + P_m(q, \nu)]. \quad (4.9)$$

This expression may be rearranged into a part which tends to a constant as $i\nu \rightarrow 0$ and a part which vanishes as ν^2 when $i\nu \rightarrow 0$. The part which tends to a constant leads to an infrared divergent contribution I given by

$$I = \frac{(i\omega - \varepsilon_f)}{[i\omega - \varepsilon_1(k)]^2 [i\omega - \varepsilon_2(k)]^2} \sum_{q, i\nu} \frac{P_m(q, i\nu)}{\det D^{-1}(q, i\nu)}. \quad (4.10)$$

Using the definition of G_c , Eq. (2.20b), and of the infrared divergent contribution a_1^* to the parameter a , we find

$$I = - \frac{\partial G_c(k, i\omega)}{\partial a} (a_1). \quad (4.11)$$

Thus the infrared divergence due to the boson propagator precisely cancels that due to the correction to the mean-

field parameter a , leaving G_c , a physical quantity, finite.

We now consider the contribution of the remaining, finite, terms to the imaginary part of the c -electron Green function. We restrict ourselves to frequencies $\omega < \varepsilon_f$ and $\omega \neq \varepsilon_1(k)$. The remaining terms have the general structure

$$\frac{F_1(k, \omega)}{[i\omega - \varepsilon_1(k)]^2 [i\omega - \varepsilon_2(k)]^2} \sum_{q, \nu} \frac{D(q, i\nu) F_2(k+q, i\omega+i\nu)}{i(\omega+\nu) - \varepsilon_1(k+q)}.$$

Here D represents some polarization bubble divided by $\det D^{-1}$, and $F_1(k, \varepsilon)$ and $F_2(k, \varepsilon)$ have no poles for $\text{Re} \varepsilon < \varepsilon_f$, and F_1 are real for real ε . Thus performing the sum on ν in the usual way, analytically continuing $i\omega \rightarrow \Omega + i\delta$, changing variables in the momentum sum to $p = k + q$, and assuming $\Omega < \varepsilon_f$ and $\Omega \neq \varepsilon_1(k)$ gives

$$\frac{-F_1(k, \Omega)}{[\Omega - \varepsilon_1(k)][\Omega - \varepsilon_2(k)]} \sum_p \frac{F_2(p, \varepsilon_1(p)) \text{Im}D(p - k, \varepsilon_1(p) - \Omega + i\delta)[f(\varepsilon_1(p)) + b(\varepsilon_1(p) - \Omega)]}{E_p}.$$

For $\Omega \ll \varepsilon_f$ the integral over the magnitude of p is restricted to $p \cong p_F$, and to leading order in Ω^2, T^2 the integral may be evaluated to give

$$\frac{F_1(k, \Omega)F_2(p_F, 0)}{[\Omega - \varepsilon_1(k)]^2[\Omega - \varepsilon_2(k)]^2} \frac{m^*}{m} \frac{\rho_0[\Omega^2 + (\pi T)^2]}{E_{p_F}} \int \frac{d^2\hat{p}}{4\pi} \lim_{\varepsilon \rightarrow 0} \frac{1}{\varepsilon} \text{Im}D[\hat{p}p_F - k, \varepsilon + i\delta]. \quad (4.12)$$

Assuming $k \cong k_F$, evaluating the angle integral as in Sec. III, and now using (4.9) and (4.12), we obtain after some algebra an expression for the $1/N$ correction to $\text{Im}G_c(k, \Omega)$, for $\Omega < \varepsilon_F$,

$$\text{Im}G_c(k, \Omega + i\delta) = \frac{1}{N} [\text{Re}G_c(k, \Omega + i\delta)]^2 n_f \frac{m^*}{m} \times \frac{\Omega^2 + (\pi T)^2}{\varepsilon_f}. \quad (4.13)$$

Equation (4.13) is the first term in a $1/N$ expansion of the full interacting c -electron Green function G_c^{full} [given by the usual formula: $(G_c^{\text{full}})^{-1} = G_c^{-1} - \Sigma_c$], where the self-energy Σ_c is order $1/N$. We thus conclude that the imaginary part of the c -electron self-energy is given by

$$\text{Im}\Sigma_c(k, \Omega + i\delta; T) = \frac{n_F}{N} \frac{m^*}{m} \frac{\Omega^2 + (\pi T)^2}{2\varepsilon_f}. \quad (4.14)$$

Several features of this result are of interest. First, note that this has the form associated with a Fermi liquid of mass m^* and Fermi temperature ε_f . Second, note that up to terms of order q_0/N , $\text{Im}\Sigma$ is momentum independent. Third, for energies of order ε_f , the scattering rate is large compared even to the hybridization gap 2Δ (see Fig. 1). For this reason we believe that the band gap obtained in the mean-field theory and sketched in Fig. 1 is an artifact of the mean-field theory, and could not be observed in a physical system.

Finally, if we argue that the low-energy piece of the real part of Σ_c (which we have not computed here) may be absorbed into a renormalization of the effective mass m^* , we may use Eqs. (4.3), (4.5), and (4.14) to write, for low energies

$$G_c(k, \Omega) = \frac{Z}{\Omega - v_f^* |k - k_f| + (i/2N) \{[\Omega^2 + (\pi T)^2]/\varepsilon_f\}}. \quad (4.15)$$

This form for G_c shows that the main effects of the electron-boson interactions on the c electrons are to (a) reduce the spectral weight of a c electron near the Fermi surface by $Z \cong m/m^*$, (b) renormalize the velocity by the same factor, and (c) contribute an inelastic scattering rate of characteristic energy ε_f . Similar ideas have been suggested by Varma¹⁹ and Fukuyama.¹²

We now study the spin polarization cloud around a given f spin by examining the correlation function

$$\chi_{\text{CF}}^z(r) = \langle M_f(0, 0) M_c(r, 0) \rangle, \quad (4.16)$$

where

$$M_f(r, t) = \sum_m m f_m^\dagger(r, t) f_m(r, t) \quad (4.17)$$

and similarly for M_c .

χ_{CF}^z may be easily computed to leading order in $1/N$ for both the lattice and the one-impurity models. By the arguments of Sec. II, the $1/N$ corrections will not change the qualitative features; we shall therefore not compute them.

To compute χ_{CF}^z in the one-impurity case it is simplest to adopt the functional integral formalism of Read and Newns.³ One introduces source terms coupling to M_f^z and $M_c^z(r)$, computes, as in Ref. 3, the free energy including source terms, and differentiates with respect to these source terms. Note that in the one-impurity case the c -electron wave vector k is a radial wave number. We must therefore use a Bessel function $j(kr)$ to convert from momentum to position space. As we are only interested in distances $r > k_f^{-1}$, and since only $k \sim k_f$ will be important, we may use the asymptotic form $j(x) \sim \cos(x)/x$, and we need not specify the order of the Bessel function. Performing the calculation leads one to evaluate the bubble shown in Fig. 9. (in which the notation is that of Ref. 3). Evaluating, we find

$$\chi_{\text{CF}}^z(r) = N \Delta' \left[\sum_{q, i\omega} \frac{j(qr)}{(i\omega - \varepsilon_q)(i\omega - \varepsilon_f + i\Delta' \text{sgn}\omega)} \right]^2. \quad (4.18)$$

Here $\Delta' = \rho V^2 a^2$; the same quantity was denoted by Δ in Ref. 3. Note that $\Delta' = \varepsilon_f/N$. From the orthonormality of the Bessel functions of different q , one may show that

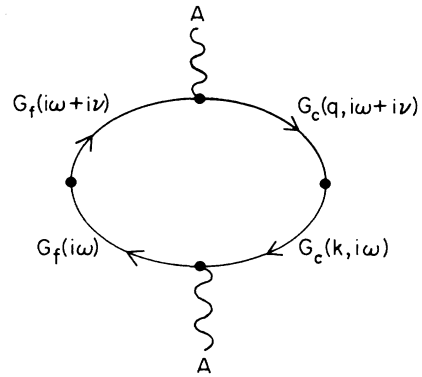


FIG. 9. Order- N diagram for the correlation function defined in Eq. (4.5), in the single-impurity case. Notation is as in Ref. 3.

$$\int d^3r \chi_{\text{CF}}^z(r) = 1. \quad (4.19)$$

There is one electron in the screening cloud.

After evaluating the frequency sum in Eq. (4.18) and taking the large- N limit as in Ref. 3, one finds that the quantity within the square brackets is given by

$$\sum_{k < k_F} \frac{\cos(kr)}{kr(\epsilon_f - \epsilon_k)}$$

for $r > k_F^{-1}$. This integral is dominated by the region $k \sim k_F$, where the denominator is $\sim \epsilon_f$. In this region we may write

$$k = k_f - \epsilon_k/v_F$$

and use $x = (k - k_F)r + r/\xi_0$ as the variable of integration. The quantity within square brackets in Eq. (4.18) becomes

$$\frac{\rho_0}{k_F r} \int_{r/\xi_0}^{\infty} dx \frac{\cos[(k_F - \xi_0^{-1})r] \cos x + \sin[(k_F - \xi_0^{-1})r] \sin x}{x},$$

where ξ_0 was defined previously and $\rho_0 = mk_F$ is the density of states. The integrals are standard. One finds that for $r/\xi_0 < 1$

$$\chi_{\text{CF}}^z(r) \sim \frac{\rho \epsilon_f}{(k_F r)^2} \ln^2 r / \xi_0, \quad (4.20)$$

while for $r/\xi_0 > 1$

$$\chi_{\text{CF}}^z(r) \sim \frac{\rho \epsilon_f}{(k_F r)^2} (\xi_0/r)^2. \quad (4.21)$$

The qualitative features are clear. In the one-impurity case the relevant energy scale is the Kondo temperature; the spin polarization cloud contains one electron and falls off rapidly—though not exponentially—for $r > \xi_0$.

We now compute the same quantity for the lattice. The relevant bubble is shown in Fig. 10. Evaluating it in the standard way gives

$$\chi_{\text{CF}}^z(r) = V^2 a^2 \left| \sum_{k < k_F} \frac{e^{ik \cdot r}}{E_k} \right|^2. \quad (4.22)$$

Integrating over all r shows that the screening cloud in the lattice case contains $\Delta/W \ll 1$ electrons, confirming the essential point of the discussion in Ref. 5. Note, however, that the relevant energy scale is Δ , not ϵ_f . The energy scale Δ is the scale over which the c -electron wave

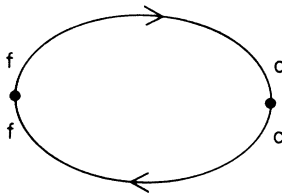


FIG. 10. Order- N diagram for the correlation function defined in Eq. (4.5) for the lattice case.

functions are modified in the lattice. This scale does not occur in the impurity problem.

We may evaluate the sum over k along the same lines as in the one-impurity problem. Note that the momentum where the denominator is minimized is k_h , not k_F (see Fig. 1). We assume $k_h r > 1$. We find

$$\chi_{\text{CF}}^z(r) \sim \frac{e^{-2r\Delta/v_F}}{(k_F r)^2} \quad (4.23)$$

[The normalization is fixed by Eq. (4.22).]

Note that the relevant length scale is v_F/Δ . This is short compared to the one-impurity length ξ_0 , but long compared to the interatomic distance k_h^{-1} . Note that the correct velocity to use in forming the length is v_F , not v_F^* .

From this it is clear that the physics of a Kondo lattice is not the same as the physics of a Kondo impurity, in agreement with the argument of Ref. 5. The local spin polarization cloud picture which applies to the impurity does not apply to the lattice. It should be pointed out that the approach of Ref. 11, which amounts to replicating the solution of the single-impurity Kondo problem over a lattice, leads to essentially the same band structure as that described by our H_0 [Eq. (2.15a)] and as that found by other authors.⁶⁻¹²

To better understand the nonmagnetic ground state in the lattice, we consider the full frequency and wave-vector-dependent susceptibility, $\chi(q, \omega)$. As discussed in Sec. III, we couple the magnetic field h to our system by adding a term hm to energy of a c or f particle of spin m . Within this assumption, the susceptibility may be calculated in the usual way. To leading order in N , the only diagram is that shown in Fig. 10, plus all possible other choices for whether the vertices involve c or f spin operators. As discussed in Sec. II, this gives the qualitatively correct results for energies much less than ϵ_f . For the imaginary part of χ and $\omega \ll \epsilon_f$ we find

$$\text{Im} \chi(q, \omega) = \frac{1}{2} \frac{\omega}{v_F^* q} \frac{1}{\epsilon_f} \Theta(v_F^* q - \omega). \quad (4.24)$$

One obtains the same result (up to terms of order m/m^*) if one couples the field to the f electrons only. This result is, of course, precisely that expected for a Fermi liquid with Fermi energy ϵ_f . This shows, among other things, that at long times (compared to ϵ_f^{-1}) the f spins are delocalized; the Pauli principle makes it unfavorable to set the f electrons in the same spin state, and it is unnecessary to form a singlet on each site.

Even though the spin degrees of freedom contributing to the enhanced susceptibility are free to move through the lattice, they will remain mostly on the f sites, because [as can be seen from Eq. (4.4) or (2.14)] the relative weight of the c -electron operator in a band-electron wave function at $k = k_F$ is only m/m^* . This has an interesting consequence for a Knight-shift experiment using an NMR resonance on a nucleus at a c -electron site—e.g., the ^9Be resonance in UBe_{13} . In such a case the Knight shift at a given site i is proportional to the square of the electron wave function at site i times the susceptibility. The susceptibility in a heavy-fermion material scales as m^*/m of a typical metallic value; the overlap between a band-1

electron at $k=k_f$ and a c -electron wave function is m/m^* ; we therefore expect that the Knight shift at a c -electron site in a heavy-fermion material would be of the same order of magnitude as in a normal metal, and would not show the mass enhancement found in χ .

We have considered the spin fluctuations; we now turn to the density-density correlation function, $S(q, \omega)$. This is the Fourier transform of $S(r, t)$, which is defined by

$$S(q, \omega) = \langle T[n(r, t), n(0, 0)] \rangle. \quad (4.25)$$

Here n is the density operator, which may be written

$$n_q = \sum_{k, m} f_{k+q}^\dagger m f_{km} + c_{k+q}^\dagger m c_{km}. \quad (4.26)$$

The diagrams for S are shown in Fig. 11 and may be easily evaluated using the results of Sec. II and the Appendix. In the Fermi-liquid regime $v_F^* q, \omega \ll \varepsilon_f$ with $y = \omega/v_F$ arbitrary we find

$$S(q, \omega) = -N\rho \frac{g(y)}{1 + F_0^s g(y)}, \quad (4.27)$$

where

$$g(y) = 1 + (y/2) \ln |(1-y)/(1+y)| + i\pi y/2\theta(1-|y|), \quad (4.28a)$$

$$F_0^s = (m^*/m)[1 - (m^*/m)(1 - n_f)^2]. \quad (4.28b)$$

The expression for F_0^s holds only in the Kondo limit, where $m^*/m(1 - n_f)^2 \ll 1$. F_0^s is the only Landau parameter not of order $1/N$ and not of order $(m^*/m)^0$. The large value of F_0^s shows that charge fluctuations are suppressed. For example, the compressibility $dn/d\mu$ is given by

$$\frac{dn}{d\mu} = \lim_{q \rightarrow 0} S(q, 0) = N\rho_0[1 + (m^*/m)(1 - n_f)^2]. \quad (4.29)$$

Thus, up to small terms, the compressibility is identical to the compressibility the c electrons alone would have. Similarly, one may study the f -density- f -density correlation function S_{ff} by using the f density and not the total density in Eq. (4.25). One finds, for the f structure factor $\text{Im}S_{ff}$, for $v_F^* q$ large and $\omega < \varepsilon_f$,

$$\text{Im}S_{ff}(q, \omega) = (1 - n_f) \text{Im}\chi(q, \omega)/N. \quad (4.30)$$

The f -change fluctuations are therefore much weaker than the f -spin fluctuations, as expected from the constraint, Eq. (2.4).

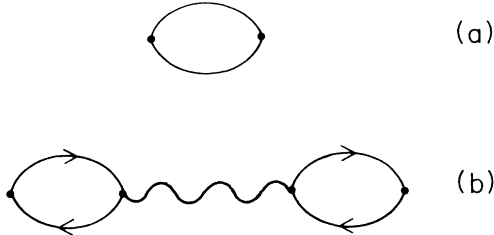


FIG. 11. Order- N diagrams for $S(q, \omega)$. The wiggly line represents the matrix of A propagators except at $\omega=0$ where λ and R propagators must be used.

We also note that the expression (4.27) for S implies the existence of a collective zero-sound mode with velocity $c^2 = F_0^s v_F^*/3$. In the presence of the long-range Coulomb interaction the mode is pushed up in energy to a “renormalized” plasma frequency of order ε_f . More details will be given in a future paper.

To summarize this section, we have shown by considering various correlation functions that the “Fermi-liquid” ground state is made up of heavy quasiparticles carrying the f spin and the c charge. Physical quantities which couple to the charge degrees of freedom, or in general to the c electrons only, are “unenhanced,” that is, do not depend on the mass enhancement m^*/m . It was previously suggested,¹⁹ by analogy with the electron-phonon problem, that many “transport” quantities are unenhanced because the interactions that lead to the heavy-fermion state are tied to the chemical potential; this leads to a strong frequency dependence and weak momentum dependence for the self-energy and vertex functions, and thus to a cancellation of m^* from transport quantities. The fact that the spin response functions are enhanced is attributed to the presence of a spin-dependent interaction. Our results, however, arise from a Hamiltonian with no spin-dependent interaction. We ascribe the fact that some quantities involve m^* and other quantities do not to the presence of two sorts of fermions (c and f) in our model, and to the constraint (2.2). Roughly, anything coupling to the spin involves the f electrons and therefore the enhanced density of states. Because of the constraint (2.2) anything coupling to the charge degrees of freedom couples only to the c electrons. Anything involving only c electrons only “sees” the enhanced density of states in subtle ways. For an example of where the mass enhancement enters into a c -electron quantity, see the discussion of the frequency-dependent conductivity in the next section.

V. FREQUENCY- AND TEMPERATURE-DEPENDENT CONDUCTIVITY $\sigma(\omega, T)$

In this section we discuss the frequency- and temperature-dependent conductivity $\sigma(\omega, T)$ for low frequencies and temperatures $\omega, T \ll \varepsilon_f$. This is a measurable quantity for which our model gives nontrivial results which are in qualitative agreement with recent experiment. It is also an illustration of how the mass enhancement enters into a transport quantity, and of how the electron-boson interaction affects a physical quantity.

Finally, the temperature dependence of σ is interesting because it is unclear whether in real systems the characteristic temperature inferred from $\sigma(T)$ is the same Kondo temperature deduced from γ, χ or the neutron linewidth, or whether it is some lower “coherence” temperature scale, determined by a different physical process than the Kondo scattering which leads to the enhanced γ, χ , etc. Our model has only one energy scale for low-energy phenomena: ε_f , which we identify with the Kondo temperature. We derive below a formula for $\sigma(T)$ at low temperatures; it seems qualitatively correct for CePd₃. Further experimental tests would, however, be of interest.

Before we can compute the conductivity, we must cou-

ple the electric field to our system. We assume the usual rule, $\nabla \rightarrow \nabla - i(e/c)\mathbf{A}$, where \mathbf{A} is the vector potential. As the f 's are dispersionless, the field couples only to the c 's. With this proviso, we may solve for the conductivity via the usual linear response. We neglect the possibility of the anomalous skin effect, and so take \mathbf{A} to depend on frequency only.

Now in a perfect lattice, the dc conductivity is infinite. To obtain sensible results, we must incorporate scattering. There are two possible sources of scattering of electrons. One is scattering of electrons off of impurities; the other is off of boson fluctuations. This latter turns out to be in some ways analogous to electron-phonon scattering. In what follows, we assume the validity of "Matthiessen's rule,"²⁰ which asserts that the resistivities due to a different scattering mechanism add. Thus if in the presence of impurities only the conductivity were σ_i and in the presence of bosons only the conductivity were σ_b , then the total conductivity would be given by

$$\sigma^{-1} = \sigma_i^{-1} + \sigma_b^{-1}. \quad (5.1)$$

Matthiessen's rule is believed to be valid when the various scattering mechanisms are not momentum dependent²⁰ and are weak. The results of Sec. II, the Appendix, and Eq. (5.2) below guarantee that the first condition is satisfied. For the second, we assume a low impurity concentration and consider only frequencies and temperatures small compared to ε_f , so that the usual Fermi-liquid phase-space effects ensure that the electron-boson scattering is weak.

We now consider the impurity contribution, $\sigma_i(\omega)$. (This will not depend on T for low T .) To compute this we must couple disorder into our system. The effects of disorder on heavy-fermion systems are various; we do not wish to enter into this subject here. For our purposes it suffices to assume that the disorder is weak and on the c -electron sites only. Then, to account for the disorder we add to the original Hamiltonian (2.4) a term

$$H_{\text{imp}} = \sum_{\substack{kk' \\ m}} V_I c_{km}^\dagger c_{k'm}. \quad (5.2)$$

We assume that this term does not affect the formal development of Sec. II in any significant way. We shall compute the effect of disorder on the c -electron Green function $G_c(k, \omega)$ via the usual Abrikosov-Gor'kov perturbation theory,²¹ assuming that the unperturbed form is that given in Eq. (2.20a). We work to leading order in N ; therefore, boson fluctuations will not enter the calculation. H_{imp} couples only to c electrons; therefore, f electrons do not enter. We need consider only the diagrams shown in Fig. 12. After solving the Dyson equation shown there we obtain the impurity-averaged Green function \bar{G}_c :

$$\bar{G}_c^{-1}(i, \omega) = G_c^{-1}(k, \omega) - \Sigma_c(k, \omega), \quad (5.3)$$

where

$$\Sigma_c(k, \omega) = \int \frac{d^3k'}{(2\pi)^3} V_I^2 \bar{G}_c(k', \omega). \quad (5.4)$$

Here, we work with real frequency ω and assume



FIG. 12. Dyson equation for the impurity averaged c -electron Green function G_c (represented by the thick line) in terms of the no-impurity Green function (represented by the thin line) and the impurity potential, here represented by the dashed line.

$\omega < \varepsilon_f$. As usual, it is the imaginary part of the self-energy Σ_c that is of interest. Making the usual ansatz,²¹

$$\text{Im}\Sigma_c(k, \omega) = \frac{i}{2\tau_i} \text{sgn}\omega, \quad (5.5)$$

and writing G_c in the convenient form,

$$G_c^{-1}(k, \omega) = \omega - \varepsilon_k - \frac{V^2 a^2}{\omega - \varepsilon_f}, \quad (5.6)$$

we may solve Eq. (5.4) for τ_i . As long as $\omega < \varepsilon_f$ we find the usual expression:

$$\frac{1}{2\tau_i} = \pi\rho V_I^2. \quad (5.7)$$

Because we have assumed that the impurity scattering is isotropic, the impurity conductivity $\sigma_i(\omega)$ is simply given by

$$\begin{aligned} \sigma_i(\omega) = e^2 \text{Im} \frac{1}{\omega} \int \int \frac{d^3k d\omega'}{(2\pi)^4} k^2 \\ \times \cos^2\theta \bar{G}_c(k, \omega + \omega') \bar{G}_c(k, \omega'). \end{aligned} \quad (5.8)$$

As usual, one evaluates this expression by performing the angle integrals and then the integral over the magnitude of k . As usual, one finds that for the integral over the magnitude of k to contribute, ω and $(\omega + \omega')$ must be of opposite sign. Further, note that the magnitude of k will be near k_F , where ε_k is large, and not near k_h , where it is small. For $\omega \ll \varepsilon_f$, (5.8) reduces to

$$\sigma_i(\omega) = \frac{ne^2}{m} \frac{\tau_i}{1 + (m^*/m)^2 \omega^2 \tau_i^2} = \frac{ne^2}{m^*} \frac{\tau_i^*}{1 + \omega^2 (\tau_i^*)^2}. \quad (5.9)$$

We have defined $\tau_i^* = (m^*/m)\tau_i$. Thus, at dc the conductivity is what one would expect for a conventional, unenhanced metal, in agreement with the ideas of Varma¹⁹ and Fukuyama.¹² Note, however, that the quantity $n = Nk_F^3/6\pi^2$ in the prefactor is the area of the Fermi surface including both c and f electrons, in agreement with Luttinger's theorem.

Our new result is that the frequency dependence is very strong. If the impurity scattering is weak, as in a good metal, the frequency $\omega^* = 1/\tau_i^*$ at which $\sigma(\omega)$ has fallen to half of its dc value may be of order 10^9 Hz (if $\varepsilon_f \sim 100$ K), a remarkably small value.

We now sketch how including scattering off of bosons modifies this result. In light of our discussion of

Mathiessen's rule above, we form the conductivity simply by adding the c -electron self-energy due to electron-boson interactions to the c -electron self-energy due to electron-impurity interactions. We note that in a Galilean-invariant theory this is not a correct procedure: identities coming from the fact that collisions conserve momentum guarantee the existence of vertex corrections that cancel the damping self-energies and lead to an infinite conductivity, in the absence of impurities even for $T \neq 0$. However, because our f electrons are dispersionless, our model is not Galilean invariant. Also, the presence of a lattice means that collisions conserve pseudomomentum, not momentum, while as shown in Sec. IV, even low-energy boson fluctuations may scatter electrons through arbitrarily large angles. Thus, umklapp processes can occur at all nonzero temperatures. For these reasons, the identities mentioned above do not apply to our model, and our procedure will give essentially the correct result. Now, using Eq. (4.14), and interpreting the imaginary part of the c -electron self-energy as a temperature- and frequency-dependent scattering rate $1/2\tau(\omega, T)$, we find

$$\frac{1}{\tau(\omega, T)} = \frac{1}{\tau_i} + \frac{1}{N} \frac{m^*}{m} \left[\frac{\omega^2 + \pi^2 T^2}{\epsilon_f} \right]. \quad (5.10)$$

Thus at $T=0$ and for $\omega < \omega_c$, with

$$\omega_c^2 = \frac{N\epsilon_f(m/m^*)}{\tau_i}, \quad (5.11)$$

the impurity scattering dominates and (5.9) applies, but for larger ω one finds

$$\sigma(\omega) \sim \frac{ne^2}{m} \frac{1}{N(m^*/m)\epsilon_f} \sim \frac{ne^2}{m} \frac{1}{W}. \quad (5.12)$$

Thus for $\omega > \omega_c$ the conductivity becomes very small (of the order of the Ioffe-Regel limit) and approximately independent of frequency. A sketch of the predicted $\sigma(\omega)$ is given in Fig. 13. The qualitative agreement with recent experiments²² is gratifying.

We now consider the case $T > 0$, $\omega = 0$. Thus, from (5.10) we write for the resistivity $\rho = \sigma^{-1}$ (after averaging 5.10 over the energies of thermally excited electrons²³)

$$\rho = \frac{m}{ne^2} \left[1/\tau + \frac{4}{N} \frac{m^*}{m} \frac{\pi^2 T^2}{3\epsilon_f} \right]. \quad (5.13)$$

Thus the coefficient of the T^2 term in the resistivity is large and scales as $(m^*/m)\epsilon_f^{-1} \sim \epsilon_f^{-2}$. To compare Eq. (5.13) with experiment it is convenient to differentiate (5.13) with respect to T^2 and make the dimensional factors explicit, obtaining

$$\frac{1}{N} \frac{m^*}{m} \frac{1}{\epsilon_f} = 5B_\mu n_{22}. \quad (5.14)$$

Here n is the carrier density in units of 10^{22} particles/cm³, ϵ_f is the Kondo temperature in units of degrees kelvin, and B_μ is the coefficient of the T^2 term in the resistivity in units of $\mu\Omega$ cm/K². For CePd₃ one finds $n_{22} = 0.35$,²² $m^*/m = 40$ [by combining data for $\sigma(\omega)$ and γ],²² while $\epsilon_f = 124$ K (taken from the neutron linewidth).²⁴ These values in combination with Eq. (5.14) imply

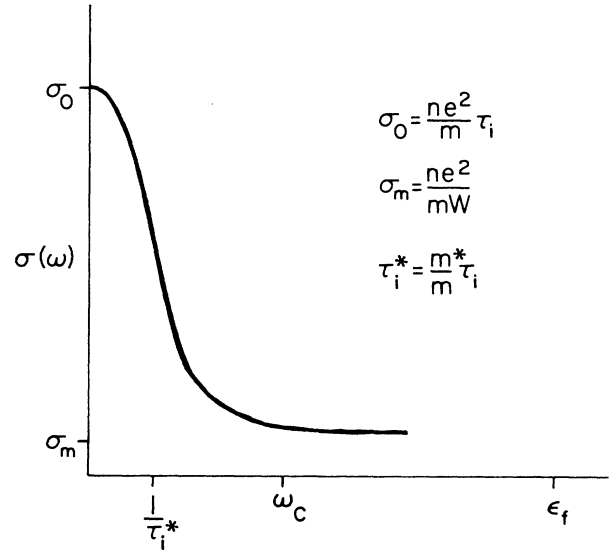


FIG. 13. Sketch of proposed form for the frequency-dependent conductivity $\sigma(\omega)$.

$B_\mu(\text{CePd}_3) = 0.12/N$; the measured value²⁴ is $\sim 7 \times 10^{-2}$; thus (5.14) seems to be correct in order of magnitude. Because we have ignored the details of Fermi-surface geometry, umklapp scattering, etc., one cannot expect (5.14) to hold precisely.

In other "heavier" heavy-fermion materials, B_μ is much larger ($B_\mu \sim 30$ in CeAl₃).²⁵ We do not have data for m^* , ϵ_f , and n . It will be interesting to see if the electron-slave-boson scattering considered here can produce such a large- T^2 coefficient in ρ .

In conclusion, we remark that the results sketched here are only valid if the following chain of inequalities holds:

$$1/\tau_i^* \ll \omega_c \ll \epsilon_f. \quad (5.15)$$

However, these conditions are equivalent to the simple condition:

$$\epsilon_f \tau_i^* \gg 1, \quad (5.16)$$

which should not be restrictive in practice.

VI. CONCLUSION

In this paper, one of several studying the low-temperature properties of the lattice Anderson Hamiltonian, we have set up the necessary formalism and established some static and low-frequency properties. We have approached the problem via a large- N expansion appropriate for a lattice. We have shown that the expansion is sensible in that the crucial constraint is preserved, infrared divergences cancel in physical quantities, and physical quantities may be computed to leading and next-to-leading order in $1/N$. We have set up formal machinery that will be useful in other papers, and we have computed various physical quantities. By way of conclusion we restate what we believe to be some of the important questions which we have addressed in this paper, along with the answers we have found.

In the limit of interest our model describes f electrons in localized orbitals far below the Fermi level, hybridizing with conduction electrons and subject to the constraint $n_f < 1$ on each site. It is unclear why, in this limit, the f spins do not order magnetically. We find, including fluctuations to order $1/N$, that the nonmagnetic ground state we have found is not unstable to ferromagnetism at any N . Other, nonsystematic approaches starting from more physical models find instability, except for very large N . The reasons for this difference are discussed in Sec. III, but the unphysical nature of our $1/N$ expansion limits the usefulness of our model in addressing the question of the competition between heavy-fermion and magnetic behavior.

The relation between the one-impurity Kondo effect and heavy-fermion behavior is an old question. We have shown that a naive extrapolation of the spin-plus-screening-cloud picture of the one-impurity Kondo effect to a lattice is incorrect, in essential agreement with the arguments of Ref. 5. We have shown that the f spins are delocalized at times long compared to ε_f^{-1} , where ε_f is given by the same formula as the single-impurity Kondo temperature.

It is almost universally agreed that some sort of "Fermi-liquid" picture of the ground state is appropriate. There has been confusion over the question of the nature of the quasiparticles. We have shown, in agreement with previous arguments from the one-impurity problem,^{2,3} that the quasiparticles carry f spin and c charge. Further, we have argued that the density-of-states enhancement will drop out of the overall magnitude (but not out of the frequency dependence) of the response to an external probe which couples either to charge degrees of freedom only or to c electrons only, whereas the enhanced density of states is present in the response to fields which couple directly to the f -spin degrees of freedom.

Further, we have shown that ε_f , the analogue of the Kondo temperature, plays the role of the Fermi energy both in the thermodynamics and in the frequency dependence of the imaginary part of the c -electron self-energy. It is also the characteristic scale for the spin-fluctuation spectrum. A larger energy scale, $\Delta = (m^*/m)^{1/2}\varepsilon_f$ is, however, the energy scale over which the c -electron wave functions are modified.

Finally, we have discussed the frequency- and

temperature-dependent conductivity, obtaining qualitative agreement with experiment and showing how the mass enhancement and the electron-boson interactions lead to nontrivial effects in the frequency dependence of a "transport" quantity.

Other papers, now in preparation, analyze the superconducting instability and the collective density-fluctuation modes.

ACKNOWLEDGMENTS

We are indebted to M. Lavagna and A. Auerbach for helpful discussions of the calculations in the Appendix. We wish to thank B. G. Kotliar for useful conversations. This research was supported by AT&T Bell Laboratories (A.J.M.) and by National Science Foundation Grant No. DMR-82-17956. We thank P. Sulewski and D. Cox for pointing out an error in the original version of Eqs. (4.14) and (5.13).

APPENDIX

In this appendix we give more details of the calculation of the boson propagators. Consider $\Sigma_{A^\dagger A}$, [Fig. 4(a)]. The analytic expression corresponding to this diagram is

$$\Sigma_{A^\dagger A}(q, i\nu) = V^2 \sum_{k, \omega} G_f(k+q, \omega+i\nu) G_c(k, i\omega). \quad (\text{A1})$$

Using the first equalities in Eqs. (2.20a) and (2.20b), we find

$$\Sigma_{A^\dagger A}(q, i\nu) = \frac{V}{a} \sum_{k, i\omega} G_m(k, i\omega) + P_m(q, i\nu) + i\nu P_1(q, i\nu). \quad (\text{A2})$$

P_1 and P_m were defined in Eqs. (2.28).

Application of Eq. (2.20b) of the text shows that the term involving G_m cancels the bare-boson energy ($\varepsilon_f - E_0$).

Clearly

$$\begin{aligned} \Sigma_{AA^\dagger}(q, i\nu) &= \Sigma_{A^\dagger A}(-q, -i\nu), \\ \Sigma_{AA}(q, i\nu) &= \Sigma_{A^\dagger A^\dagger}(q, i\nu) = P_m(q, i\nu). \end{aligned}$$

Thus, we may write

$$D^{-1}(q, i\nu) = \begin{pmatrix} i\nu[1 - P_1(q, i\nu)] - P_m(q, i\nu) & -P_m(q, i\nu) \\ -P_m(q, i\nu) & -i\nu[1 - P_1(-q, -i\nu)] - P_m(q, i\nu) \end{pmatrix}. \quad (\text{A3})$$

We now consider the determinant of this matrix. It is

$$\det D^{-1}(q, i\nu) = -(i\nu)^2 [1 - P_1(q, i\nu)][1 - P_1(q, -i\nu)] + i\nu P_m(q, i\nu) [P_1(q, i\nu) - P_1(q, -i\nu)]. \quad (\text{A4})$$

However, after some algebra one may show

$$P_1(q, i\nu) - P_1(q, -i\nu) = -\frac{i\nu}{a^2} P_f(q, i\nu). \quad (\text{A5})$$

Substitution of (A5) into (A4) yields Eq. (2.26) of the text.

We now evaluate—for small ε —the polarization bub-

bles P_1 , P_m , and P_f which appear in the boson propagators.

We consider imaginary parts first. For $\varepsilon < \varepsilon_f$, crossband transitions are not energetically possible; one may restrict oneself to the lower band. The calculation of P_1 will serve as an example. P_1 is defined by

$$P_1(q, iv) = \frac{-V}{a} \sum_{k, i\omega} G_f(k, i\omega) G_m(k+q, i\omega + iv). \quad (\text{A6})$$

Evaluating the Matsubara sum in the usual way, and analytically continuing $iv \rightarrow \varepsilon + i\delta$, and taking the imaginary part yields

$$\text{Im}P_1(q, \varepsilon + i\delta) = \frac{V}{a} \sum_k \frac{Va}{E_{k+q}} U_k^2 \delta(\varepsilon + \varepsilon_1(k) - \varepsilon_1(k+q)) \times [f(\varepsilon_1(k)) - f(\varepsilon_1(k+q))]. \quad (\text{A7})$$

For $\varepsilon \ll \varepsilon_f$, one knows that all energies are small and all wave vectors are close to k_F , then $u_k^2 = 1$. Also, $\text{Im}P_1(q, \varepsilon + i\delta) = 0$ unless

$$q > \varepsilon/v_F^*, \quad (\text{A8})$$

where

$$v_F^* = \frac{d\varepsilon_1(k)}{dk} = k_F/m^* = (m/m^*)v_F.$$

We may now perform the integral over the angle between k and $k+q$. Using Eq. (2.2b), we find

$$\text{Im}P_1(q, \varepsilon + i\delta) = V^2 \int dk \frac{k^2}{4\pi^2} \frac{f(\varepsilon_1(k)) - f(\varepsilon + \varepsilon_1(k))}{E_{k+q} \left| \frac{d\varepsilon_1(k+q)}{d\varepsilon_{k+q}} \right| \frac{kq}{m}} \Theta(q - \varepsilon/v_F^*) \Theta(2k_F - q). \quad (\text{A9})$$

The factors in the denominator come from the δ function and are to be evaluated at $\varepsilon_1(k+q) = \varepsilon_1(k) + \varepsilon$. Also, for $|k| \cong k_F$, $d\varepsilon_1(k)/d\varepsilon_k = m/m^*$.

Expanding (A9) for small ε , we find

$$\text{Im}P_1(q, \varepsilon + i\delta) = \frac{1}{2} V^2 \left[\frac{m^*}{m} \right]^2 (\varepsilon/\varepsilon_{k_F})(m/k_F q) \times \Theta(qv_F^* - \varepsilon) \Theta(2k_F - q).$$

Now, defining

$$n_f = (1 + \varepsilon_f/\rho_0 V^2)^{-1}, \quad (\text{A10a})$$

$$\alpha = q_0 n_f / \rho_0 W, \quad (\text{A10b})$$

$$\beta = \Theta(qv_F^* - \varepsilon) \Theta(2k_F - q), \quad (\text{A10c})$$

and using Eq. (2.18), we find

$$\text{Im}P_1(q, \varepsilon + i\delta) = -\frac{\varepsilon}{\varepsilon_f} \frac{1}{8} \frac{n_f}{(1-n_f)^2} \alpha \left[1 - \frac{\alpha}{2} - \frac{n_f \alpha}{4} \right] \beta + O(\alpha^3). \quad (\text{A11a})$$

Similarly,

$$\text{Im}P_m(q, \varepsilon + i\delta) = -\frac{\varepsilon}{8} \frac{n_f}{1-n_f} \alpha \left[1 - \frac{\alpha}{2} - \frac{n_f \alpha}{4} \right] \beta + O(\alpha^3), \quad (\text{A11b})$$

$$\text{Im}P_m(q, \varepsilon + i\delta) = \frac{m^*}{m} \frac{\varepsilon}{8} \frac{n_f}{1-n_f} \alpha \left[1 - \frac{\alpha}{2} - \frac{n_f \alpha}{4} \right] \beta + O(\alpha^3). \quad (\text{A11c})$$

The real parts of these bubbles are more difficult to compute; we consider only $\varepsilon=0$, and we work to leading and next-to-leading order in the small parameter q_0 . Computing each bubble requires evaluating an integral over the loop wave vector \mathbf{k} . In each case the dominant contribution to the integral over the magnitude of k comes from the ‘‘heavy’’ part of the lower band, where $k_h < k < k_F$ (see Fig. 1). Now by Eq. (2.18) $|k_F - k_h|$ is of order q_0 . We shall exploit this fact in what follows.

We now turn to the details of the calculation, using again P_1 as an example. Beginning from Eq. (A6), evaluating the Matsubara sum, continuing $iv \rightarrow \varepsilon + i\delta$, taking the real part, and setting $\varepsilon=0$ gives

$$\text{Re}P_1(q, 0) = V^2 \int \frac{d^3k}{(2\pi)^3} \frac{u_k^2}{E_{k+q}} \frac{f(\varepsilon_1(k)) - f(\varepsilon_1(k+q))}{\varepsilon_1(k) - \varepsilon_1(k+q)} - \frac{u_k^2}{E_{k+q}} \frac{f(\varepsilon_1(k))}{\varepsilon_1(k) - \varepsilon_2(k+q)} + \frac{v_{k+q}^2}{E_k} \frac{f(\varepsilon_1(k+q))}{\varepsilon_1(k+q) - \varepsilon_2(k)}. \quad (\text{A12})$$

Combining terms and changing integration variables where necessary leads to

$$\text{Re}P_1(q, 0) = +V^2 \int \frac{d^3k}{(2\pi)^3} \frac{f(\varepsilon_1(k))}{E_k} \frac{(E_k - \varepsilon_f + \varepsilon_{k+q})}{[\varepsilon_{k+q} - \varepsilon_1(k)][\varepsilon_f - \varepsilon_1(k)] - V^2 a^2}. \quad (\text{A13})$$

Our assumed quadratic form for ε_k implies

$$\varepsilon_{k+q} = \varepsilon_k + \frac{kq\mu}{m} + \frac{q^2}{2m}, \quad (\text{A14})$$

where μ is the angle between k and q .

After making the substitution (A14), Eq. (A13) may be recast to read

$$\begin{aligned} \text{Re}P_1(q,0) = & +V^2 \int \frac{d^3k}{(2\pi)^3} f(\varepsilon_1(k)) \\ & \times \left[\frac{u_k^2}{V^2 a^2} + \frac{2u_k^4 E_k}{V^2 a^2} \frac{m}{kq} \frac{1}{\mu + q/2k} \right]. \end{aligned} \quad (\text{A15})$$

The angle integrals are now trivial. The integral over the magnitude of k is simplified by the fact that

$$u_k^2 \cong \frac{V^2 a^2}{\varepsilon_k^2}, \quad |k| < k_h. \quad (\text{A16})$$

The dominant contribution to the integrals thus comes from the region $k_F > k > k_h$, where one may make the following approximations:

$$u_k^2 = 1, \quad (\text{A17a})$$

$$E_k = \varepsilon_k. \quad (\text{A17b})$$

One then finds

$$\text{Re}P_1(q,0) = \frac{1}{a^2} \int_{k_h}^{k_F} dk \frac{k^2}{2\pi^2} \left[1 + \varepsilon_k \frac{m}{kq} \ln \left[\frac{1+q/2k}{1-q/2k} \right] \right]. \quad (\text{A18})$$

This integral may be evaluated. Note that the dominant contribution to the second term is of order q_0 relative to the first, and that the dominant contribution to the integral over the second term comes from the variation of ε_k .

We may set $k = k_h$ in the remainder of the second term, with errors of order q_0^2 . By making use of (2.18) and (2.23), we find

$$\text{Re}P_1(q,0) = \frac{n_f}{1-n_f} \left[1 + \frac{\alpha}{4} + \frac{\alpha}{8} F(q/2k_F) \right]. \quad (\text{A19a})$$

Here

$$F(x) = \frac{1}{x} \ln \left| \frac{1+x}{1-x} \right|.$$

Note that $1 - n_f \ll 1$, thus $\text{Re}P_1 \gg 1$.

The real parts of the other bubbles may be evaluated similarly. We find

$$\text{Re}P_F(q,0) = \frac{n_f}{1-n_f} \frac{m^*}{m} \varepsilon_f \left[1 + \frac{\alpha}{3} + \frac{\alpha}{12} F(q/2k_F) \right], \quad (\text{A19b})$$

$$\text{Re}P_M(q,0) = -\frac{\varepsilon_f}{4} \frac{n_f}{1-n_f} \alpha F(q/2k_F). \quad (\text{A19c})$$

All expressions are correct only for small q_0 .

Finally, we consider the determinant of the matrix $D^{-1}(q, \varepsilon + i\delta)$, in the limit $\varepsilon \rightarrow 0$. After analytically continuing Eq. (2.27), we find

$$\det D^{-1}(q, \varepsilon + i\delta) = \varepsilon^2 \{ [1 - P_1(q, \varepsilon + i\delta)][1 - P_1(q, -\varepsilon - i\delta)] + P_m(q, \varepsilon + i\delta) P_F(q, \varepsilon + i\delta) / V^2 a^2 \}. \quad (\text{A20})$$

Now the real parts of all polarization bubbles considered here are proportional to a constant plus order ε^2 , while the imaginary parts are proportional to ε plus order ε^3 . Thus we may use the previous results of this appendix to write $\det D^{-1}$ up to order ε^4 :

$$\text{Im} \det D^{-1}(q, \varepsilon + i\delta) = \frac{\alpha\beta}{8(1-n_f)^2} \frac{\varepsilon^3}{\varepsilon_f} \left[1 - (1-n_f)^2 - \alpha n_f (1-n_f/6 - n_f^2/4) - \frac{n_f^2 \alpha}{12} F(q/2k_F) \right], \quad (\text{A21})$$

$$\text{Re} \det D^{-1}(q, \varepsilon + i\delta) = \frac{\varepsilon^2}{(1-n_f)^2} \left[1 + n_f \alpha / 2 + \frac{1}{4} \alpha n_f (1-n_f) F(q/2k_F) \right]. \quad (\text{A22})$$

*Present address: AT&T Bell Laboratory, 600 Mountain Avenue, Murray Hill, NJ 07974-2070.

¹P. A. Lee, T. M. Rice, J. W. Serene, L. J. Sham, and J. W. Wilkins, *Comments Condensed Matter Phys.* **128**, 99 (1986).

²P. Coleman, *Phys. Rev. B* **29**, 3035 (1984).

³N. Read and D. M. Newns, *J. Phys. C* **16**, 3273 (1983).

⁴S. E. Barnes, *J. Phys. F* **6**, 1375 (1976).

⁵P. Nozières, *Ann. Phys. (Paris)* **10**, 19 (1985).

⁶N. Read, D. M. Newns, and S. Doniach, *Phys. Rev. B* **30**, 384 (1984).

⁷P. Coleman, in *Proceedings of the 8th Taniguchi Symposium on the Theory of the Valence Fluctuating State*, Vol. 62 of

Springer Series in Solid State Science, edited by T. Kasuya and T. Saso (Springer-Verlag, New York, 1985); P. Coleman, Ph.D. thesis, Princeton University, 1984.

⁸A. Auerbach and K. Levin, *Phys. Rev. Lett.* **57**, 877 (1986); *Phys. Rev. B* **34**, 3524 (1986).

⁹T. M. Rice and K. Ueda, *Phys. Rev. Lett.* **55**, 995 (1985).

¹⁰C. M. Varma, W. Weber, and L. J. Randall, *Phys. Rev. B* **33**, 1015 (1986).

¹¹H. Razafimandimby, P. Fulde, and J. Keller, *Z. Phys. B* **54**, 111 (1984).

¹²H. Fukuyama, in *Proceedings of the 8th Taniguchi Symposium on the Theory of the Valence Fluctuating State*, Vol. 62 of

- Springer Series in Solid State Science*, edited by T. Kasuya and T. Saso (Springer-Verlag, New York, 1985).
- ¹³A. J. Heeger, in *Solid State Physics*, edited by F. Seitz and D. Turnbull (Academic, New York, 1969), Vol. 21.
- ¹⁴S. Coleman, in *Proceedings of the 19th International School of Subnuclear Physics*, edited by A. Zichichi (Plenum, New York, 1981).
- ¹⁵N. Read, *J. Phys. C* **18**, 2651 (1985).
- ¹⁶P. W. Anderson, *Basic Notions of Condensed Matter Physics* (Benjamin/Cummings, London, 1984).
- ¹⁷J. M. Luttinger, *Phys. Rev.* **119**, 1153 (1960).
- ¹⁸P. Coleman, *Phys. Rev. B* **28**, 5255 (1983).
- ¹⁹C. M. Varma, in *Proceedings of the 8th Taniguchi Symposium on the Theory of the Valence Fluctuating State*, Vol. 62 of *Springer Series in Solid State Science*, edited by T. Kasuya and T. Saso (Springer-Verlag, New York, 1985).
- ²⁰N. W. Ashcroft and N. D. Mermin, *Solid State Physics* (Holt, Reinhart and Wilson, Philadelphia, PA, 1976), p. 323.
- ²¹A. A. Abrikosov, L. P. Gor'kov, and I. E. Dzyaloshinski, *Methods of Quantum Field Theory in Statistical Physics*, edited by R. A. Silverman (Dover, New York, 1975).
- ²²B. C. Webb, A. J. Sievers, and T. Mihalisin, *Phys. Rev. Lett.* **57**, 1951 (1986).
- ²³See, e.g., P. B. Allen and R. Silbergliitt, *Phys. Rev. B* **9**, 4733, 1974.
- ²⁴J. M. Lawrence, J. D. Thompson, and Y. Y. Chen, *Phys. Rev. Lett.* **54**, 2537 (1985).
- ²⁵G. R. Stewart, *Rev. Mod. Phys.* **56**, 755 (1984).